Spring 5-12-2017

One-Pot Syntheses and Characterizations of “Click-able” Polyester Polymers for Potential Biomedical Applications

James F. Beach II
Pittsburg State University, jbeach@gus.pittstate.edu

ONE-POT SYNTHESES AND CHARACTERIZATIONS OF "CLICK-ABLE" POLYESTER POLYMERS FOR POTENTIAL BIOMEDICAL APPLICATIONS

A Thesis Submitted to the Graduate School
in Partial Fulfillment of the Requirements
For the Degree of
Master of Science in Polymer Chemistry

James F. Beach II

Pittsburg State University

Pittsburg, Kansas

May, 2017

ONE-POT SYNTHESES AND CHARACTERIZATIONS OF "CLICK-ABLE" POLYESTER POLYMERS FOR POTENTIAL BIOMEDICAL APPLICATIONS

James F. Beach II

APPROVED:

Thesis Advisor _____
Dr. Santimukul Santra, Department of Chemistry

Committee Member _____
Dr. Irene Zegar, Department of Chemistry

Committee Member _____
Dr. Charles Neef, Department of Chemistry

Committee Member _____
Dr. Petar Dvornic, Department of Chemistry

Committee Member _____
Dr. Neil Snow, Department of Biology

ACKNOWLEDGEMENTS

First, I would like to extend thanks to PSU's Polymer Chemistry Initiative and the College of Education for their financial assistance throughout the pursuit of my graduate degree.

Thank you to our research collaborator, Dr. Richard Gross of the Rensselear Polytechnic Institute, for the donation of the Novozyme-435 enzyme catalyst used to perform the synthesis detailed in this thesis.

I would like to thank Dr. Jian Hong of the Kansas Polymer Research Center for his aid in the operation and data processing of various instruments used over the course of this project.

I would like to thank my lab mates Shoukath Sulthana, Shuguftha Naz, and Tanuja Tummala for their aid and instruction of various cell culturing tasks and biological assays performed in this thesis.

I would like to thank all my committee members for donating their time and energy in the revision and editing of this thesis. You have all aided me significantly during my undergraduate and graduate degrees at PSU, and I am incredibly appreciative that you all have offered to serve on this committee.

Lastly, I wish to express my sincerest gratitude to both Dr. Santimukul Santra and Dr. Tuhina Banerjee for accepting me as a member of their lab and giving me the opportunity to perform research. The guidance you have both provided throughout my graduate degree has been invaluable, and is something I will carry with me wherever life takes me beyond this degree.

ONE-POT SYNTHESES AND CHARACTERIZATIONS OF "CLICK-ABLE" POLYESTER POLYMERS FOR POTENTIAL BIOMEDICAL APPLICATIONS

An Abstract of the Thesis by
James F. Beach II

In this study, a linear polyester polymer was designed using polyethylene glycol, sorbitol, glutaric acid and 4-pentynoic acid as monomers. The synthesis was carried out using standard melt polymerization technique and catalyzed by Novozyme-435, an enzyme suitable for polymerization of biocompatible compounds. The progress of the reaction was monitored with respect to time and negative pressure, with samples being subjected to standard characterization protocols. Polymer with high molecular weight and water solubility were chosen for further modification into folate-functionalized polymeric nanoparticles for targeted drug delivery to cancer cells. This was achieved by employing a solvent diffusion method, wherein the polymer can be simultaneously converted into water-soluble nanoparticles and therapeutic agents (Taxol) and imaging dyes (DiI) can be encapsulated. The efficacy of this delivery system was gauged by treating LNCaP and PC3 prostate cancer cells with the drug and dye-loaded nanoparticles and assessing the results of the treatment. The results were analyzed by cytotoxicity (MTT) assays, drug release studies, and confocal and fluorescence microscopy. The experimental results collectively show a nanoparticle that was biocompatible, target-specific, and successfully initiated apoptosis in an in-vitro prostate cancer cell model.

Keywords: Nanoparticle · Cancer · Polyester · Click chemistry · Nanomedicine

TABLE OF CONTENTS

LIST OF FIGURES

FIGURE # PAGE

CHAPTER I

INTRODUCTION

To the average person, the world “polymer” brings only a few things to mind. It likely invokes images of conventional, mundane objects: desks, chairs, bottles, and the like. However, the meaning and impact within this word goes much deeper than household items and manufacturing materials. The field of polymer science has affected the way of life (for better and worse) for most life forms on this planet for the greater part of the last century. This trend is likely to continue, as the demand for polymer-based solutions to many of the world’s material problems increases. This demand compels polymer science to permeate into disciplines that have never been thought possible. Fortunately, this cross-over has become a reality with the technological and intellectual strides that have been made in modern times.

One such area polymer science has invaded is the field of biomedicine and nanotechnology. Conventional treatments for the world’s more worrisome diseases have become somewhat dated and are occasionally detrimental to the overall well-being of the patient. Current cancer treatment methods often leave a patient in a more compromised state of health than the cancer alone. Chemotherapeutics and radiation therapy occasionally fail to impede the disease’s progress while simultaneously subjecting the patient to undesirable side effects (hair loss, nausea, loss of appetite, etc.). Fortunately, polymer science has risen to answer the call for new treatment methods in the unorthodox form of polymeric nanoparticles.

Polymeric nanoparticles (PNPs) are a relatively new development in the field of medicine, and polymer science in general. Biologically compatible polymers (typically dendritic polymers) can be synthesized using commercially available chemicals to create new compounds with biomedical applications. However, there are many caveats to creating a suitable polymer for medicinal applications. These compounds must be innately non-toxic to the host upon administration, as well as degrade and pass through the body without complication. The polymers must also be able to overcome any innate hydrophobicity to be converted onto a nanoparticle solution. The resulting particles must then exhibit enough stability to be deemed appropriate for the encapsulation of therapeutics and optical dyes.

The subject of this thesis focuses on the synthesis of one such polymer, utilizing polyethylene glycol as the primary bulk of the polymeric backbone to improve the hydrophilicity of the polymer, as water solubility is necessary in polymers that may see implementation in biological systems. The other monomers used were glutaric acid, sorbitol, and 4-pentynoic acid. Glutaric acid and sorbitol were chosen for their already well-established biocompatibility *in-vivo*, the former being a natural byproduct of various metabolic processes, and the latter being the reduced form of d-glucose.[1,2] The 4-pentynoic acid was chosen to ensure an alkyne (C≡C) surface functionality when converted to polymeric nanoparticles. This allows for the polymeric nanoparticles to be immediately modified via “click” chemistry, wherein azide-terminated folic acid can be reacted with these surface groups to serve as selective ligands.

Following synthesis and modification of the polymeric nanoparticle solution, the anticancer drug Paclitaxel (Taxol) and DiI optical dye was encapsulated within the polymer for this drug delivery system. These polymeric nanoparticles were incubated with LNCaP and PC3 prostate cancer cells to analyze the results of treatment via cytotoxicity assay. LNCaP prostate cancer cells express a prostate-specific membrane antigen (PSMA) that displays high affinity for

folic acid, which is lacking in PC3 cells. From this, it can be gauged whether the proposed system can selectively treat cancers expressing this receptor, or if this formulation needs revising as the project moves toward in-vivo studies.

CHAPTER II

LITERATURE REVIEW

A History of Polymers

A polymer can be defined as a large macromolecule consisting of a massive number of repeat units called monomers.[3,4] Polymers have a ubiquitous presence in the lives of all organisms on our planet, whether they occur naturally (DNA, lignin) or are created synthetically (plastics, nylons). The first strides into the field of polymer science were made by German chemist Hermann Staudinger, who documented the existence of these macromolecules in 1920.[5] Staudinger's work with rubbers led him to believe there may be something more contributing to the large molecular weights that he was obtaining experimentally. He was convinced that rubber and other large molecular weight compounds (cellulose, proteins, etc.) were comprised of long chains of repeating units with covalent linkage.[6,7] He proposed these thoughts and findings in his landmark 1920 paper, which was met with widespread criticism from his contemporaries.

At the time, the widely-held belief was that unusually high molecular weights (above 5,000 g/mol) were due to the aggregation of molecules into a colloidal structure, and that covalent linkage between two identical molecules was impossible.[6] It wasn't until the late 1930s that Staudinger could further validate his claims into scientific proof, with the help of some like-minded scientists. Austrian-American chemist Herman Mark was able to support Staudinger's macromolecular theory with his work on the x-ray diffraction of fibers, which provided

significant evidence for existence of numerous covalent linkages within a sample.[8] The American chemist Wallace Carothers, who had long been a pioneer in organic chemical synthesis, contributed strongly to the Staudinger's claims with his discoveries of polyesters and nylon (polyamides).[9] The work of these scientists helped propel Staudinger's theory into a solid foundation for polymer science, and allowed the discipline to develop into the widespread and economically important industrial and research fields that exist today.

Biodegradable Polymers

The synthesis of biodegradable polymers hearkens back to the late 1980s, when non-industrial applications of polymers were first being explored.[10,11] The earliest conducted research saw scientists attempting to integrate natural polymer derivatives (polysaccharides, lipids, etc.) into the fields of agriculture, medicine, and ecology.[10-12] The aim was to create polymers with readily hydrolysable backbones, which would degrade naturally within various environments (physiological pH, nitrogen in soil) in order to facilitate exogenous processes (nitrogenation, soil stabilization).[10] However, it was found that natural polymers were not very susceptible to degradation, making their potential for use in biological and other natural fields limited. This has compelled researchers to design and synthesize new polymers, using monomer compounds that, at the time, were quite unconventional. Compounds like sugar derivatives, amino acids, and alcohols were used to synthesize polymers that were not only biodegradable, but biocompatible in certain cases.[12]

In particular, synthetic polyester biopolymers came to prominence in this field due to their ease of synthesis, high molecular weight, biocompatibility and degradation.[10,12] Initial research in this synthesis saw wide usage of polylactic acid (PLA) as the standard for biocompatible and biodegradable polyester synthesis.[13] PLA is derivative of lactic acid, a

compound produced naturally in all animals as a byproduct of various metabolic processes (Krebs and Cori cycles, gluconeogenesis).[14] As such, this greatly increases the odds of PLA-based polymers being successful when introduced into a biological system. Naturally, the synthesis of biocompatible polyesters has become more intricate, using dicarboxylic acids and diols as monomers to make completely original compounds. Ventures into custom-made biopolymers have seen their greatest results in hyperbranched and dendrimer synthesis, unique polymers that have demonstrated remarkable potential in the field of medicine and biological sciences.[15]

Biomedical Applications of Polymers

In the field of medicine, polymers have seen success as vehicles for site-specific drug delivery, biosensors, and gene therapy.[16-18] They perform this role by being converted into polymeric nanoparticle solution, bestowing them with new and enhanced properties. Nanoparticles are particles of 1-1000 nm diameter into which dendritic and certain linear polymers can be converted when dispersed in the appropriate solvent. Once dispersed, these molecules orient themselves into nano-sized geometric shapes (spheres, rods, globular), wherein the polymer backbone comprises the inner matrix and certain functional groups (polar) are on the outer surface of the particle.[16,19] This is controlled in the initial synthesis of the monomer, where the compound containing the desired surface functionality is kept in molar deficiency or excess, depending on the synthetic method and type of polymer (e.g. linear polymers will form a matrix via crosslinking), to the other reactants.[16,19] Additionally, the chosen surface functionality is often a polar compound (primary amines, alcohols) due to their hydrophilicity, which make them available for further modification.[16,19]

The creation of the polymer matrix of the nanoparticle creates a network of pockets, not unlike a spider web, that possess unique properties. This intramolecular space is created

due to electrostatic repulsion (e.g. carbonyl oxygens) or pendant groups present in the polymeric backbone, as well as the innate hydrophobicity of the aliphatic backbone.[19,20] In the case of linear polymers, this intramolecular space is generated in some part due to light crosslinking between adjacent molecules. This internal space can be utilized for the encapsulation of various small molecules, typically hydrophobic drugs and optical dyes, within the nanoparticle. The nanoparticles act as a freighter, protecting its cargo from outside interference and preserving their activity en route to a cell or tumor.[16-20] This feature is of significant interest in medical research, and is changing the way researchers approach disease treatment.

Nanoparticles and Their Role in Cancer Treatment

The ability of nanoparticles to encapsulate small molecules has seen them rising to prominence in the discovery of new disease treatment methods, particularly for cancer.[17-20] In this regard, nanoparticles display great potential to move away from systemic treatment and towards targeted drug delivery. This is accomplished by encapsulating drugs and other compounds (dyes, MRI contrast agents) within the nanoparticle, which are released upon cellular uptake. The uptake is facilitated by receptor-mediated invagination of the nanoparticle, after which the polymer matrix is degraded by the abnormally low pH (approx. 4-5) of the tumor cytosol.[18-20] This releases the cargo molecules directly into the cell, simultaneously administering the drug and allowing for monitoring of the cell's size as apoptosis occurs.[16-20] This gives the nanoparticle the multimodality of both a therapeutic and diagnostic agent, something seldom seen in the realm of conventional cancer treatment.

Nanoparticles can be further modified by bonding ligands to their surface functional groups, which allow for specific receptor targeting. This ensures that the encapsulated

compounds only enter cells of interest. This is often a necessary modification, as many of the default surface functionalities (carboxylates and hydroxyls) would display electrostatic repulsion with the overall negative charge of the cell membrane.[16-20] This allows the nanoparticle to act as a Trojan horse, deceiving the tumor into absorbing its toxic payload. In many cancers, there is an overexpression of folic acid (folate) receptors in the outer membrane, which is lacking in healthy cells.[21] As the name implies, these receptors show a high affinity for folic acid, which can be used against the tumor cell while leaving neighboring healthy tissues unaffected.[21] Nanoparticles can be decorated with targeting ligands by reacting the surface functional group of unmodified nanoparticles with a functional group of the desired (and usually modified) ligand molecule.[16-20] This conjugation is usually accomplished via carbodiimide (CDI) cross-linker (amine, hydroxyl, or carboxyl decorated nanoparticles) or "click" (alkyne decorated nanoparticles) chemistries and their respective counterpart functionalities on the ligand.[22-23]

Cytotoxicity Assays

Successful conjugation of the nanoparticles and their targeting molecule are confirmed by various biological assays, in which the nanoparticles are incubated with cancer cells.[16-20] These assays are performed to confirm the selectivity of the nanoparticles, as there should be no display of cytotoxicity in the control cells that lack folate receptors. One such test is the MTT (3-(4,5-dimethylthiazol-2-yl)-2,5-diphenyltetrazolium bromide) cytotoxicity assay. This assay calculates the degree of cytotoxicity by utilizing MTT as a colorimetric indicator. MTT is a yellow tetrazole compound which, when catalyzed by mitochondrial reductase, undergoes reduction to formazan, a violet crystalline compound **(Figure 1)**.[24]

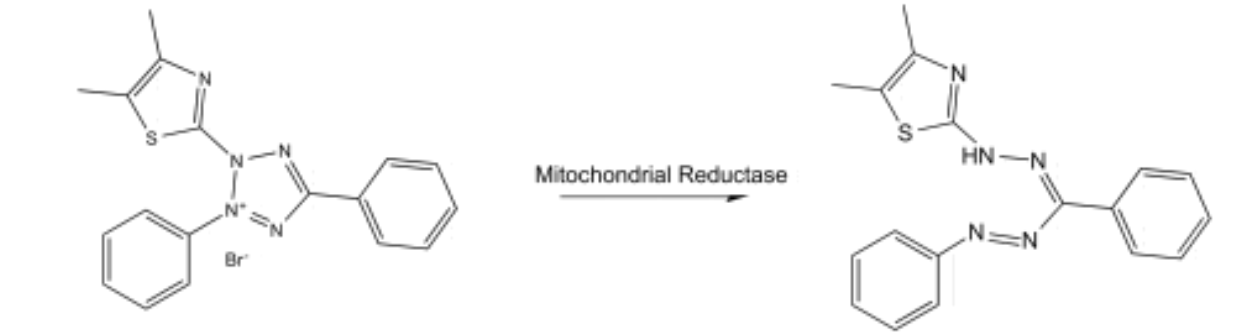

Figure 1: The Reduction of MTT to Formazan

Mitochondrial reductase is a NAD(P)H-dependent oxidoreductase produced during typical cellular metabolism.[25] As such, the amount of this enzyme produced in a cell is dependent on its overall health, as can be qualitatively determined by its ability to reduce MTT.[24-25] Cells undergoing apoptosis will produce much lower levels of mitochondrial reductase and, subsequently, lower levels of formazan. The degree of cytotoxicity can be determined quantitatively by analyzing the absorbance spectra (at 500-600 nm) of the cells with respect to formazan production.[24-25]

CHAPTER III

RESULTS AND DISCUSSION

1. Polymer Synthesis and Characterizations

Synthesis: The polymer was synthesized using compounds known to individually exhibit high levels of biocompatibility and hydrophilicity. Additionally, one of the reagents (4-pentynoic acid) was chosen to create surface functionalities amenable to "click" chemistry once the polymer is converted to a nanoparticle suspension.[19-20] For the synthesis of the polymer, melt polymerization with an enzyme catalyst (Novozyme-435) was utilized. The selected reagents were sorbitol, glutaric acid, 1000 MW polyethylene glycol (PEG-1000) and 4-pentynoic acid in a molar ratio of 1: 2: 1: 0.5, respectively. This was done to ensure equimolarity of the polyols while providing the glutaric acid in excess, which would increase the odds of esterification occurring between these three compounds. The 4-pentynoic acid was provided in molar deficit to reduce the chances of it reacting with primary hydroxyl groups, as that would terminate polymerization on one end of the growing chain. A separate reaction utilizing 300 MW polyethylene glycol (PEG-300) was also performed, maintaining the same molar equivalents as the first. A proposed scheme of the reaction and resulting polyester polymer is shown in Figure 2. Samples of each polymer that had undergone 48 hours of reaction were subjected to standard chemical and polymeric characterizations, as detailed in the following sections.

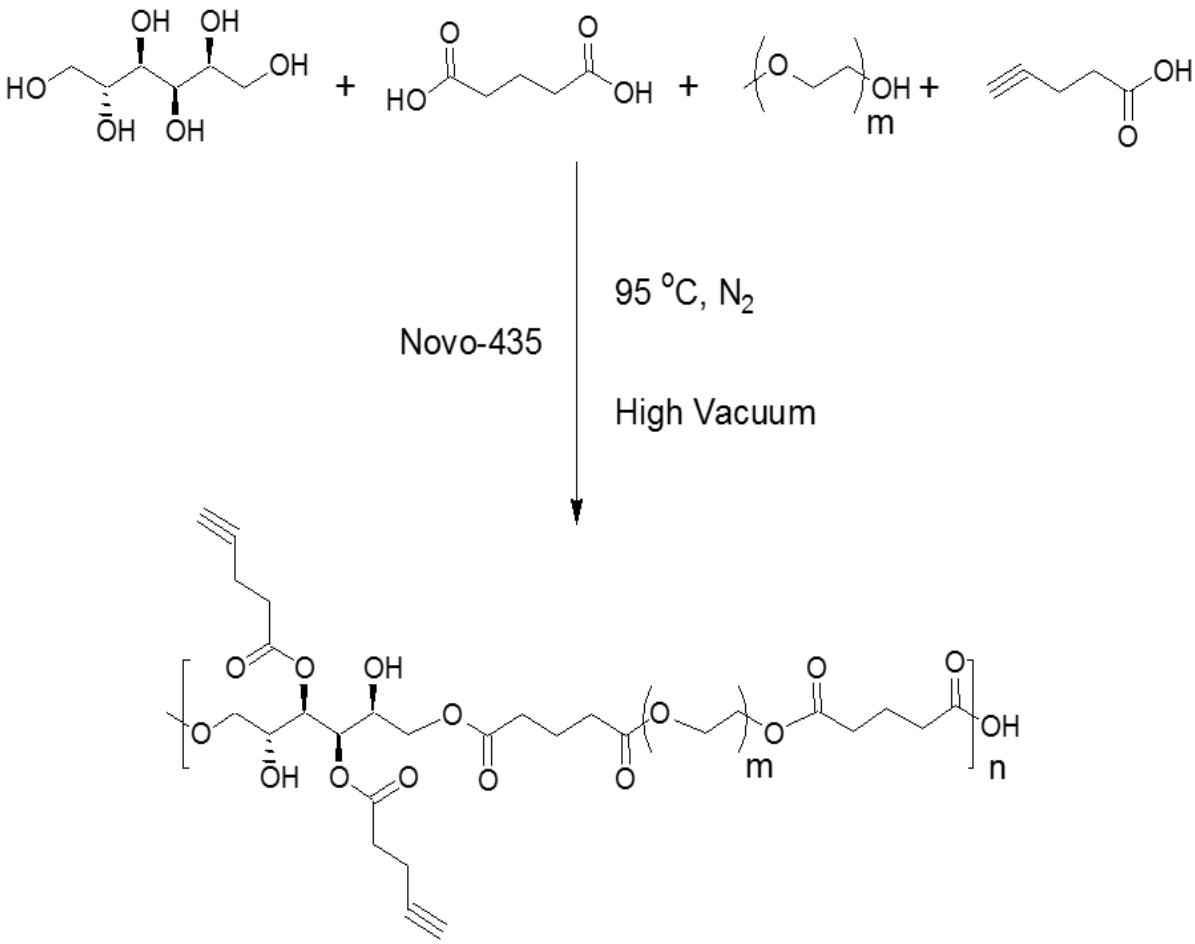

Figure 2: Reaction scheme for the polymerization of a "Click-able" polyester polymer

^{1}H NMR: The proton NMR spectra for each of the starting compounds and polymer samples are shown in Figures 3-5. The TMS reference peak was observed at 0 ppm. The solvent peak for DMSO-d_6 was observed as a singlet around 2.5 ppm in each of the spectra, except in the 4-pentynoic acid spectrum, which was performed in chloroform-d (7.25 ppm).

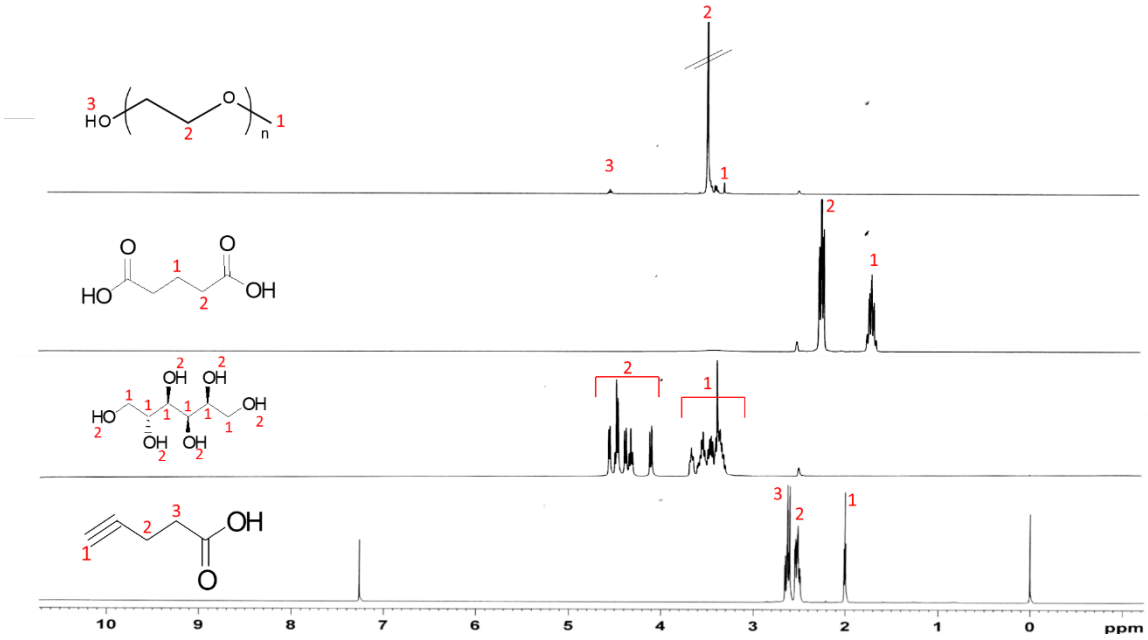

Figure 3: ^{1}H NMR Spectra of Starting Compounds

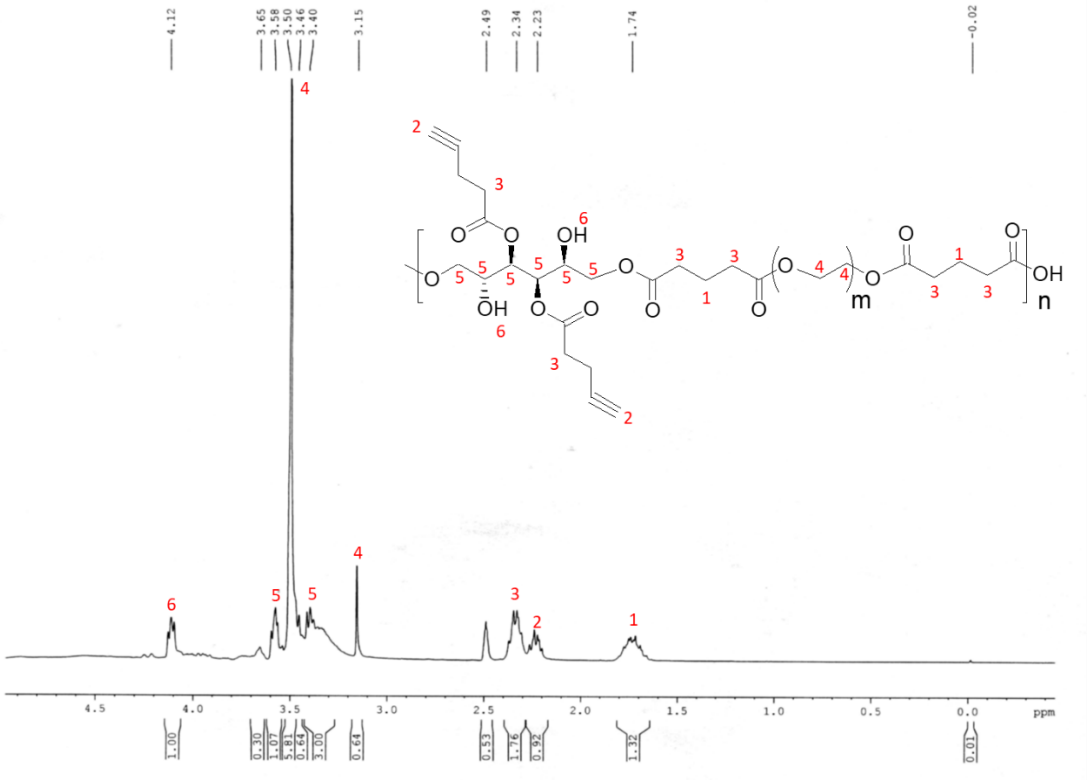

Figure 4: ^{1}H NMR Spectrum of PEG-300 Polyester Polymer

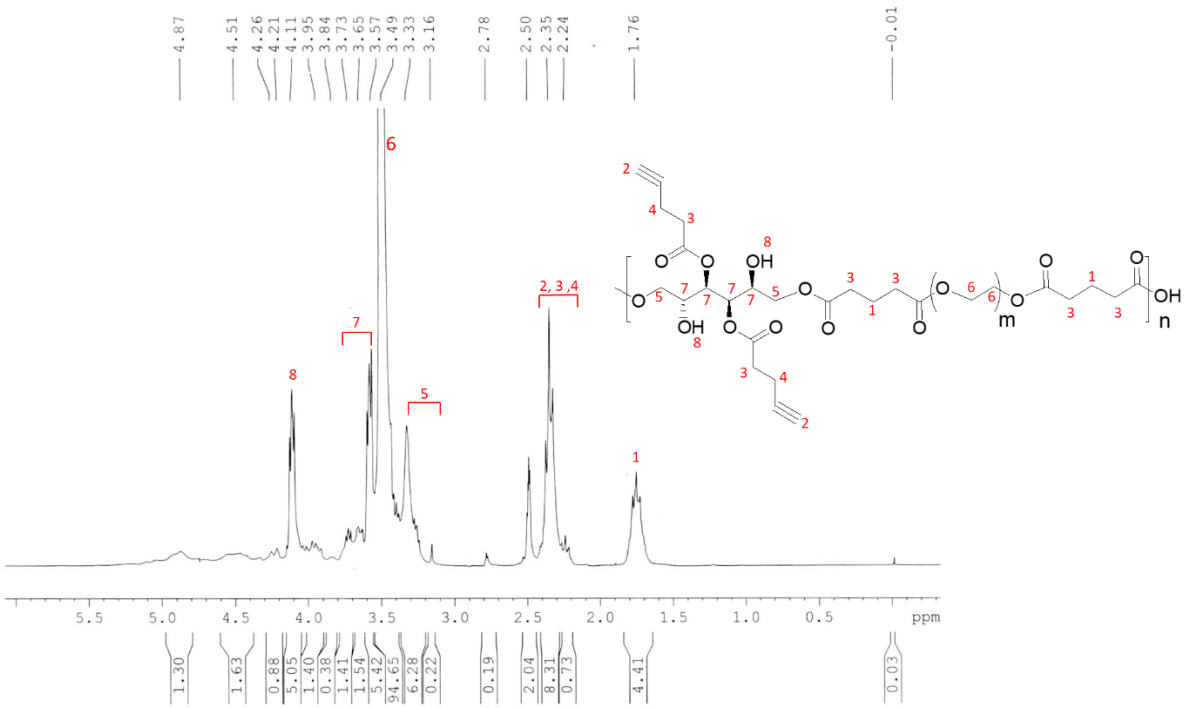

Figure 5: ^{1}H NMR Spectrum of PEG-1000 Polyester Polymer

The peak at 3.50 ppm representing the protons in both PEG-300 and PEG-1000 were seen in the spectra for both polymers. This peak inserted itself between the peak clusters of the aliphatic (3.3-3.7 ppm) and hydroxyl (4.1-4.5 ppm) protons found in sorbitol. The methylene protons of glutaric acid and 4-pentynoic acid were observed at 1.74 ppm and 2.34 ppm. The alkyne peak of 4-pentynoic acid was observed at around 2.23 ppm in the polymer spectra.

The spectra of the polymers showed the major functionalities of the monomer compounds present within their overall structure. Polymers, due to their large molecular weights and the presence of multiple protons in the same environments within the repeat units, tend to manifest as much broader and irregular peaks compared to those seen in non-polymeric compounds. This can cause overlapping or masking of some of the weaker signals in the spectra, which makes them more difficult to isolate and analyze. Generally, the positions of distinct

peaks from the monomer compounds are used as a marker for location in the polymer's spectra, as they should appear in a similar region.

It is also worth noting that in the spectra for 4-pentynoic acid and glutaric acid, the characteristic peak for the carboxyl hydrogen (around 10-12 ppm) was not observed. This likely is due to the hygroscopic nature of the deuterated solvents, as they are can absorb moisture if precautionary measures are not taken during preparation of the samples and transfer to the NMR tube. The acidity of these protons means that they are exchangeable with those of the water contaminant, which may cause the carboxylic acid proton peak to diminish or disappear.[27] This is supported by the presence of the very shallow and broad band at 3.40 ppm in the glutaric acid spectra, which is indicative of water in the sample.

^{13}C NMR: The carbon-13 NMR spectra for the monomer and polymer samples are shown in Figures 6-8. The solvent peak for DMSO-d_6 manifests as a strong multiplet at 40 ppm in each of the spectra.

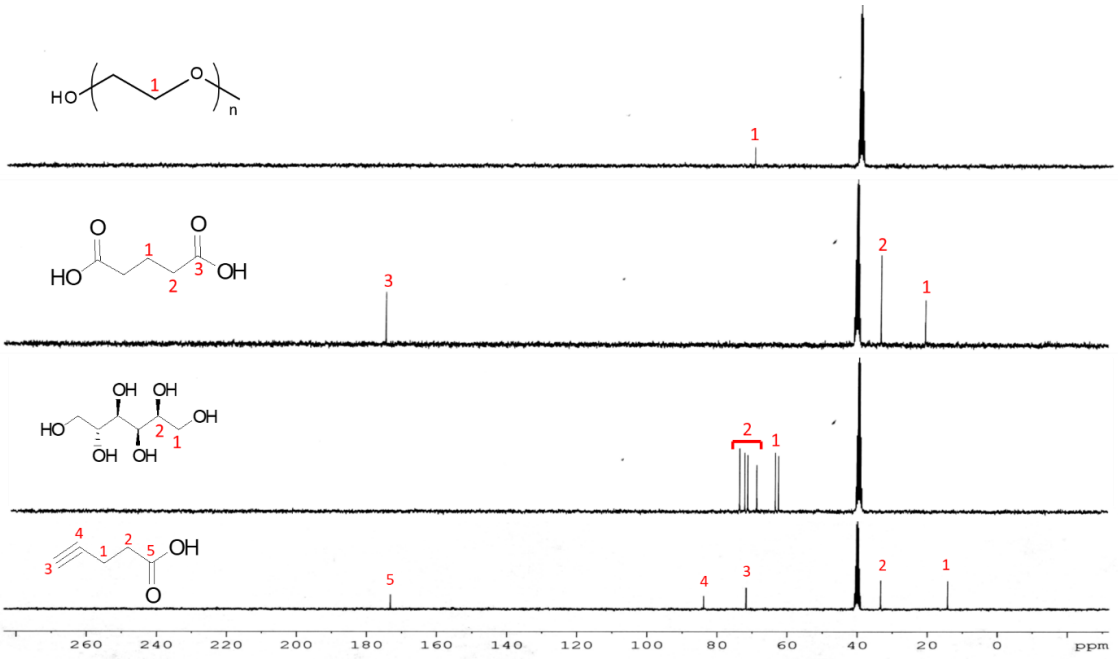

Figure 6: ^{13}C NMR Spectra of Starting Compounds

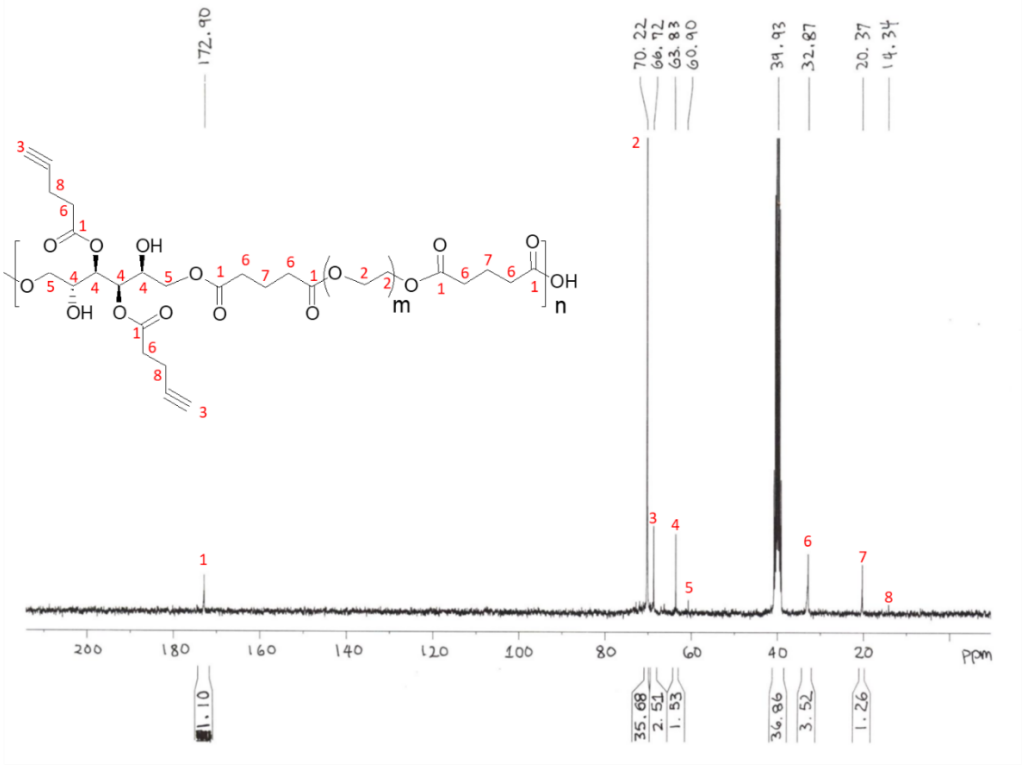

Figure 7: ^{13}C NMR Spectrum of PEG-300 Polyester Polymer

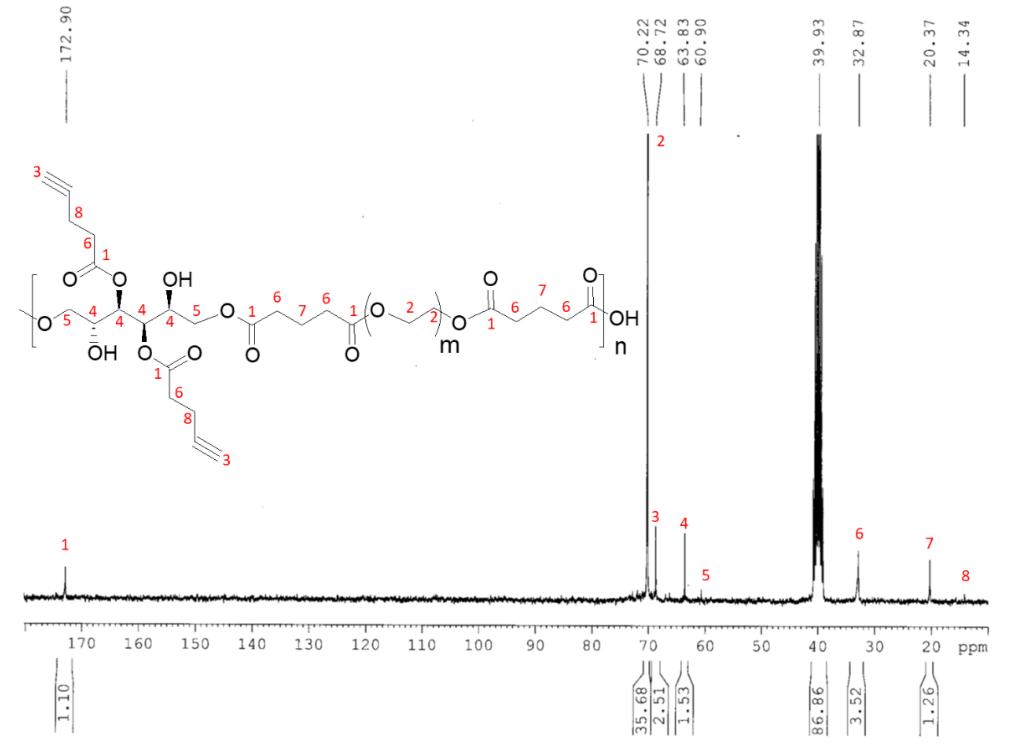

Figure 8: ^{13}C NMR Spectrum of PEG-1000 Polyester Polymer

The peaks of the carbonyl carbons in both acid monomers were observed at 173 ppm. The peak around 70 ppm was indicative of the carbons of both PEG compounds. The peak at 68.7 ppm represented the terminal alkyne carbon of the 4-pentynoic acid. The peaks around 61 and 64 ppm represented the aliphatic carbons of sorbitol. The peak around 33 ppm represented the carbon adjacent to the carbonyl groups in both glutaric acid and 4-pentynoic acid. Finally, the carbon adjacent to the alkyne bond in 4-pentynoic acid was observed around 14 ppm. As with the proton NMR, the relative shifts of the peaks in the individual compounds were used as a landmark to locate similar peaks in the spectra of the polymer.

FT-IR: The FT-IR spectra for the monomer compounds is shown in Figure 9, while spectra for the PEG-300 and PEG-1000 polyester polymers can be seen in Figures 10 and 11, respectively.

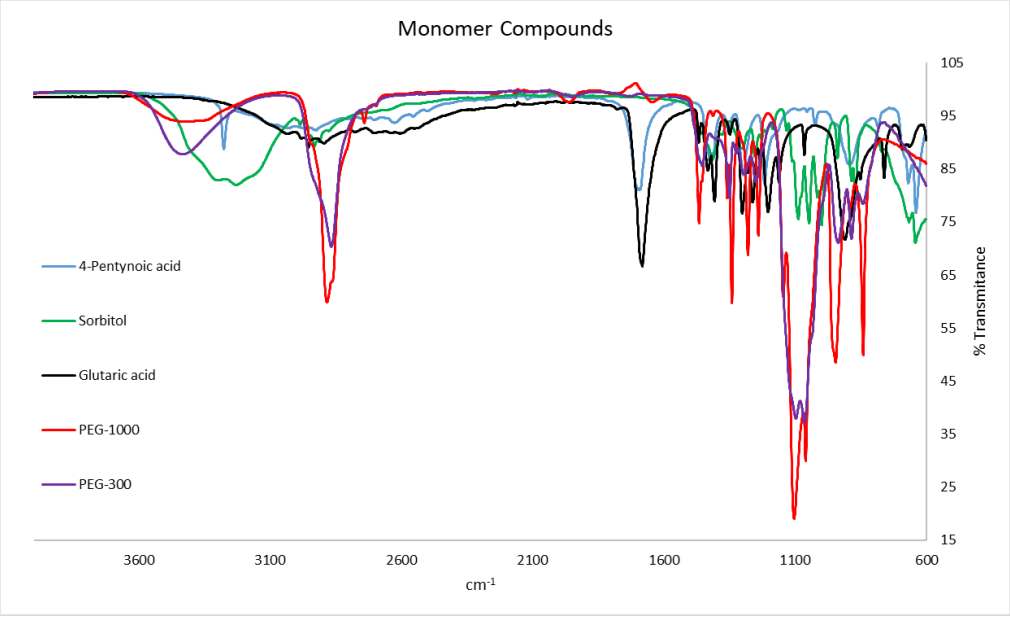

Figure 9: FT-IR Spectra of Starting Compounds

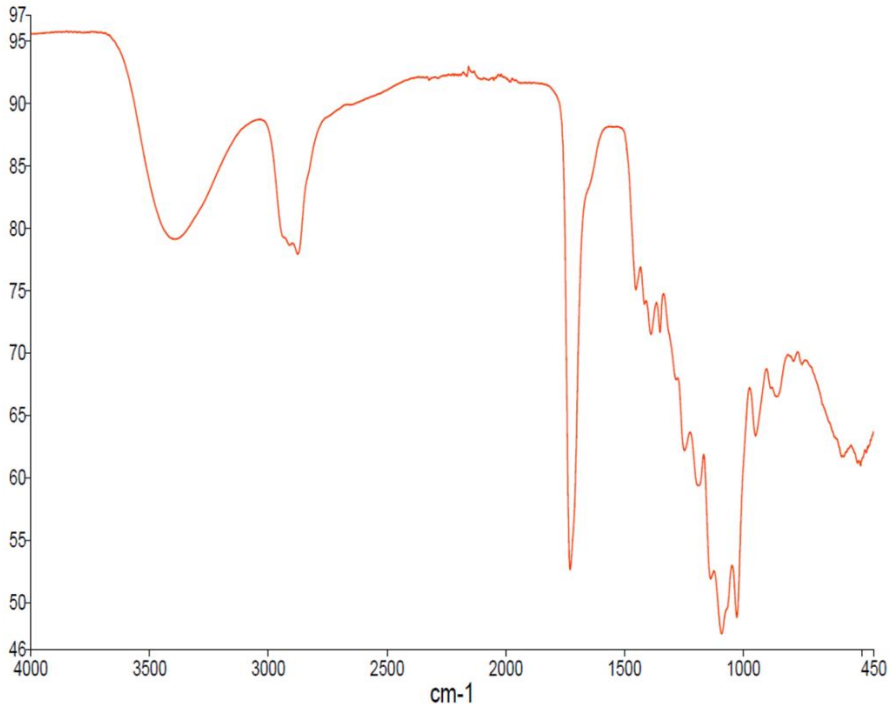

Figure 10: FT-IR Spectrum of PEG-300 Polyester Polymer

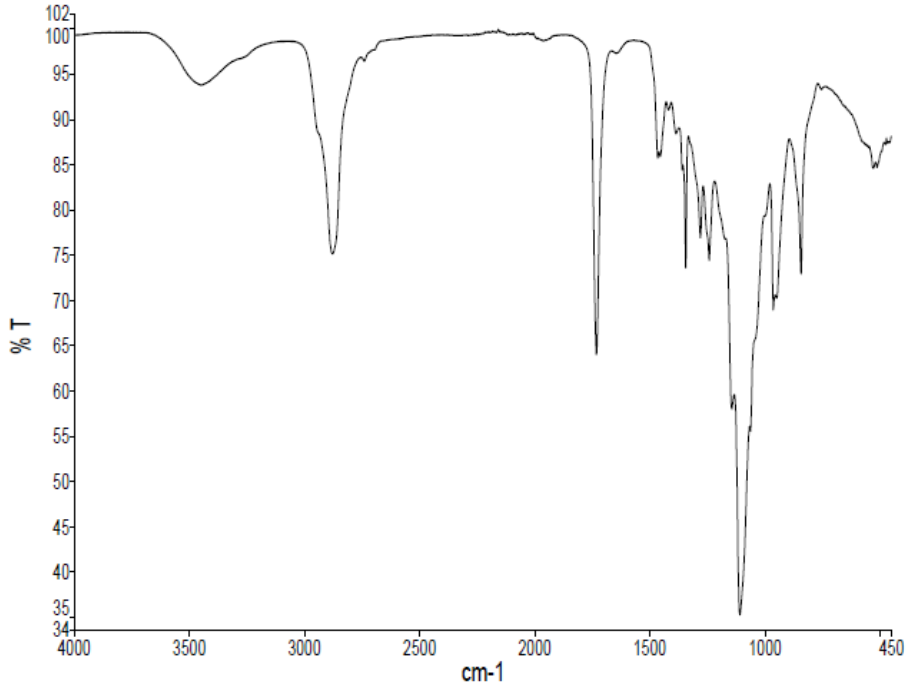

Figure 11: FT-IR Spectrum of PEG-1000 Polyester Polymer

As observed in the FT-IR spectra, the distinctive strong peak at around 1735 cm^{-1} represented the ester carbonyl (C=0) bond, suggesting successful polymerization of the monomer compounds. This was further confirmed by the strong peak at 1130 cm^{-1}, indicating C-O stretching from both the ester and aliphatic ether linkages (from PEG). The strong peak at 2880 cm^{-1} represented the alkyl (C-H) bond stretching, as was expected in aliphatic polymers. The broad, shallow stretching from 3340-3650 cm^{-1} was indicative of the hydroxyl (O-H) groups of the sorbitol. Faint alkyne stretches were observed near 2200 cm^{-1} (CΞC) and 3265 cm^{-1} (C-H). These peaks lacked the distinct sharpness of standard terminal alkynes, but this weakness was attributed to the molar deficit (around 25% molar deficit, as compared to the highest molar equivalent reagent) to which the 4-pentynoic acid was used in the synthesis, and may be masked by the frequencies of other nearby bond stretches.

MALDI-TOF: The results of MALDI-TOF scanning can be seen below in Figures 12 and 13. The polymers were cast in a matrix comprised of TA30 solution and 2,5-dihydroxybenzoic acid and analyzed using Bruker's "flexcontrol" MALDI imaging software.

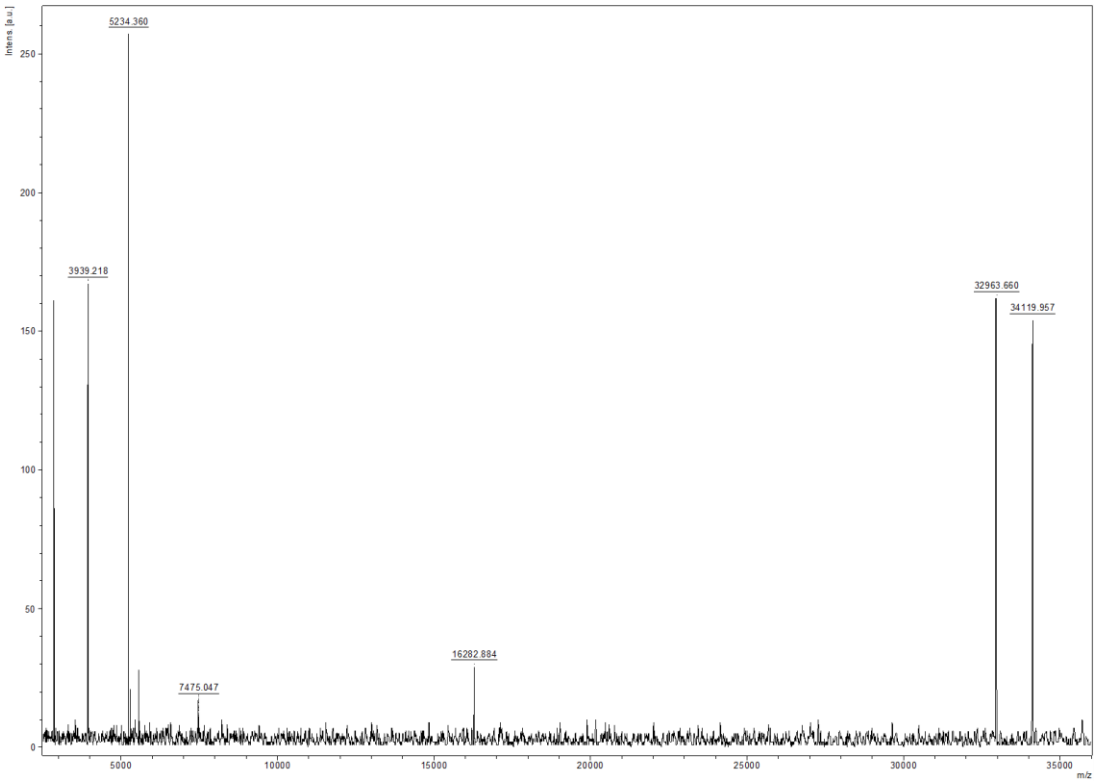

Figure 12: MALDI-TOF of PEG-300 Polyester Polymer

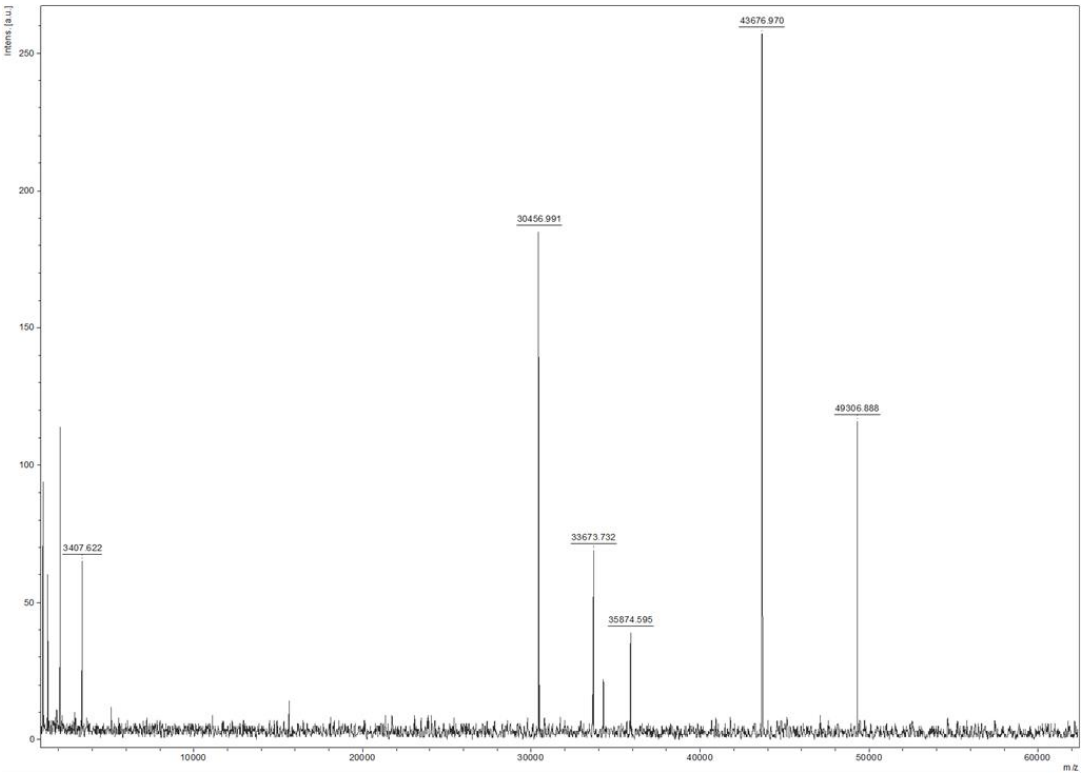

Figure 13: MALDI-TOF of PEG-1000 Polyester Polymer

Large fragments with Mn values of 34,100 and 43,670 were observed for the PEG-300 and PEG-1000 polymer samples, respectively. To calculate the potential Mw, the polydispersity index (PDI) of 1.8 obtained from GPC was used, which is typical of synthetic polyester polymers.[28] Using this PDI value and the corresponding equation (PDI= Mw/Mn), a Mw of 61,380 and 88,740 was obtained for the PEG-300 and PEG-1000 polymer samples, respectively. Both the PEG-300 and PEG-1000 polyester polymers showed polymers with high molecular weight. This exceeded the literature values of polyester polymers synthesized in a similar manner, but it was suspected it would have no detrimental effects to its function due to its water solubility.

GPC: The results of gel permeation chromatography of each polymer samples can be seen in Figures 14 and 15.

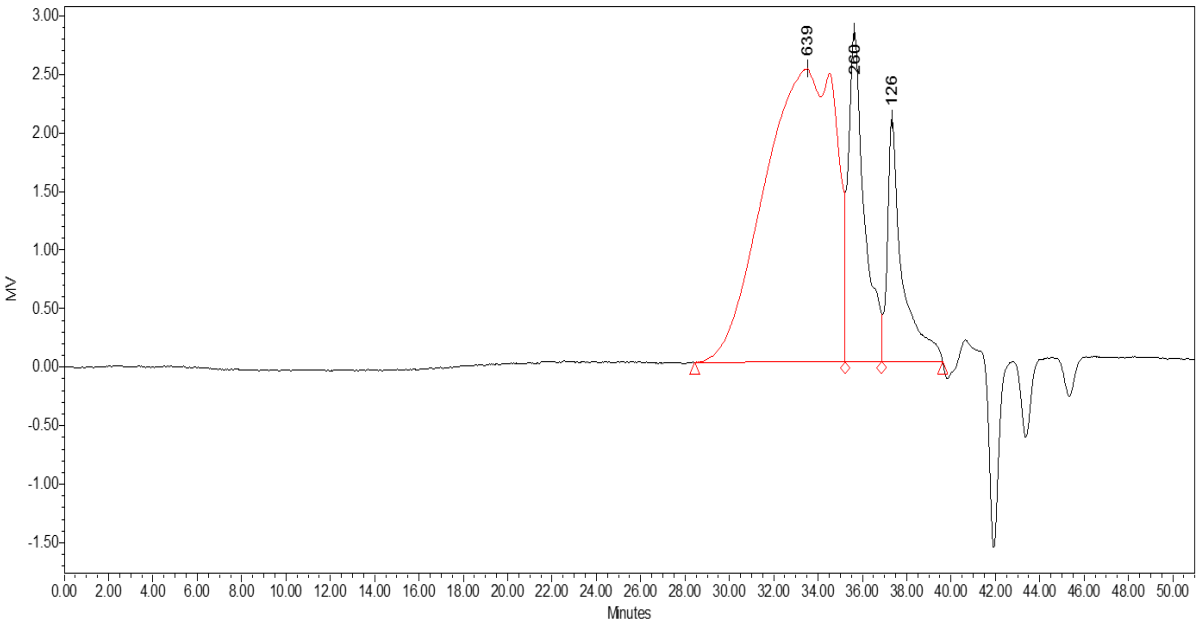

Figure 14: GPC of PEG-300 Polyester Polymer

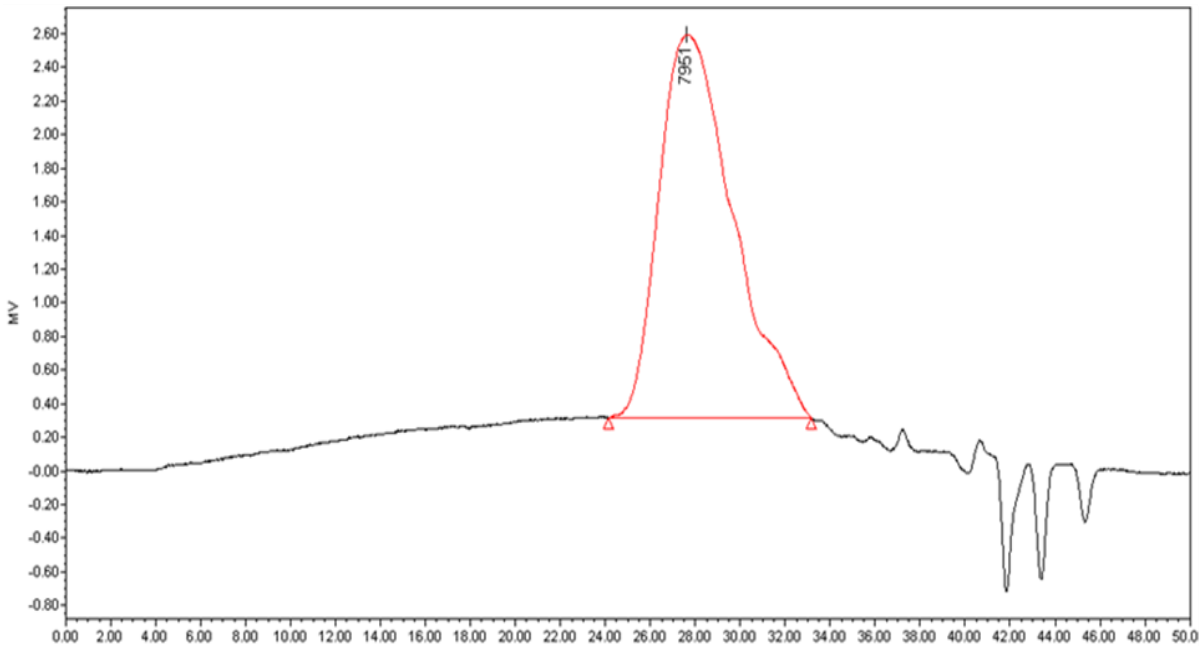

Figure 15: GPC of PEG-1000 Polyester Polymer

As seen in the spectra, both samples displayed elution of high molecular weight product at around 32 minutes and 28 minutes for the PEG-300 and PEG-1000 polymers, respectively. This suggested that the PEG-1000 polymer was higher in molecular weight when subjected to equal reaction time (also confirmed by MALDI). This was also supported by the presence of additional peaks in the PEG-300 spectra, which appear between 35-37 minutes of elution time. This may be indicative of smaller weight fractions or oligomers present in the sample. It also was determined that each sample had a PDI around 1.8.

TGA: The results of thermogravimetric analysis for the two samples are shown in Figures 16 and 17.

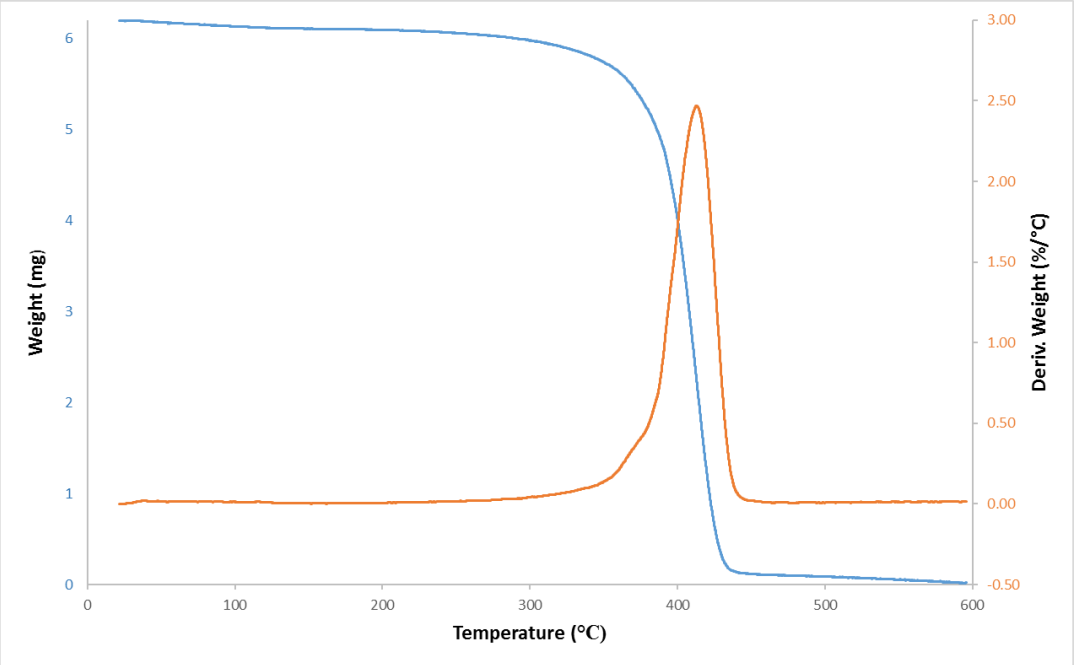

Figure 16: TGA of PEG-300 Polyester polymer

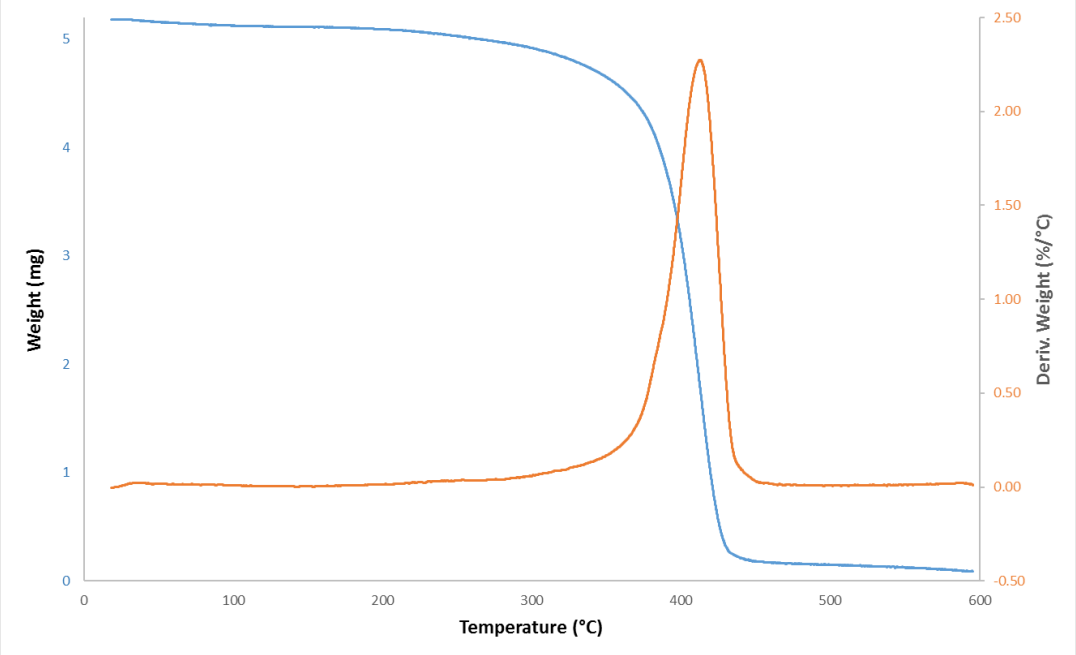

Figure 17: TGA of PEG-1000 Polyester Polymer

Both polymer samples exhibited degradation (10% weight loss) at temperatures around 370°C. This degradation temperature was slightly higher than is typical of polyesters, which tend

to degrade around 350°C. This could be attributed to light cross-linking occurring between the carboxyl groups in the pendants and the hydroxyl groups in the sorbitol component, which would increase degradation temperatures. Regardless, the TGA results suggest that the polymer will easily remain thermostable at biological temperatures (37°C) and with no threat of thermal degradation.

DSC: The results of differential scanning calorimetry for the polymer samples are shown in Figures 18 and 19.

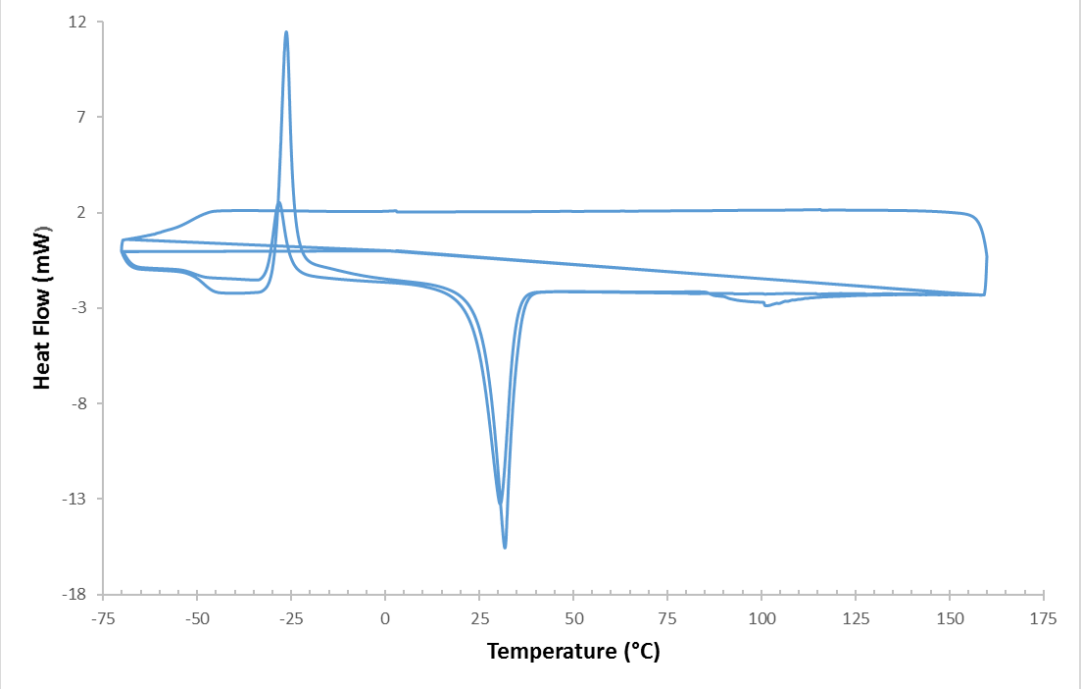

Figure 18: DSC Curve of PEG-300 Polyester Polymer

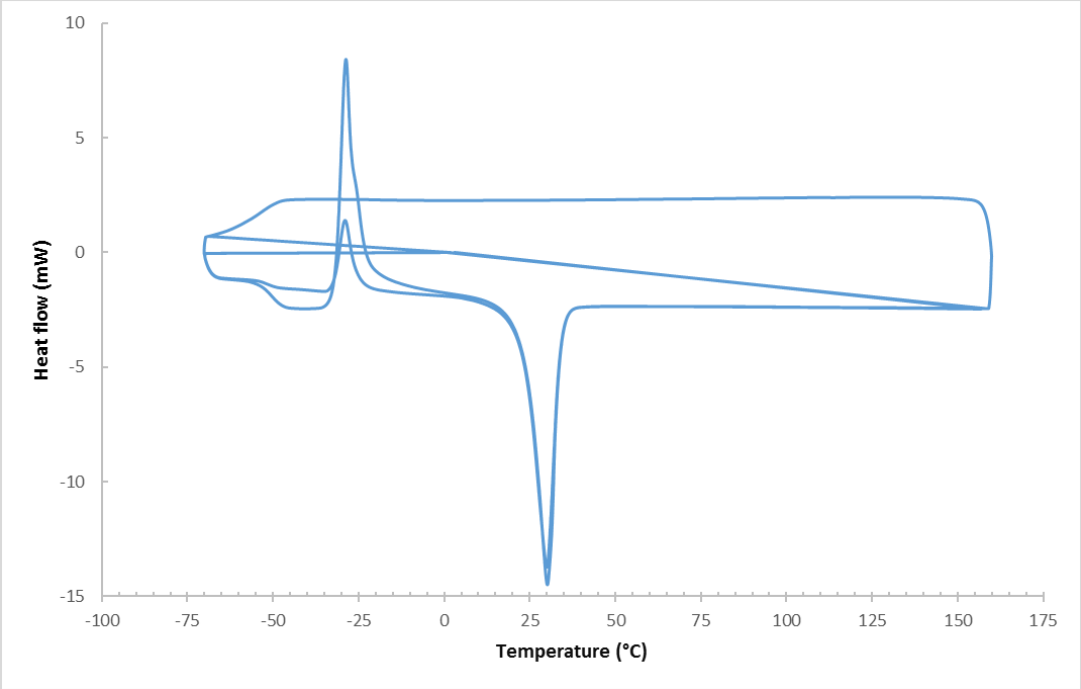

Figure 19: DSC Curve of PEG-1000 Polyester Polymer

Both polymer samples displayed glass transition temperatures (T_g) at approximately -50°C, crystallization temperatures (T_c) around -29°C, and melting temperatures (T_m) around 31°C. This showed characteristics of a polymer possessing low degrees of crystallinity (or somewhat amorphous). The low T_g and T_c are likely due to the presence of PEG in each of the polymers, as the large number of ether linkages in the polymer backbone confers chain flexibility.[26]

2. Polymeric Nanoparticle Synthesis and Characterization

Following characterization, the polymers were converted into polymeric nanoparticles (PNPs) for drug and dye encapsulation utilizing a "solvent diffusion" method. This method utilizes rigorous mixing to force the polymer and the hydrophobic cargo to interact, encouraging the dye molecules to be encapsulated within the hydrophobic pockets of the polymer matrix.

Characterizations for these nanoparticles are included in the following sections, and a scheme detailing the full nanoparticle synthesis and modification can be seen in Figure 20.

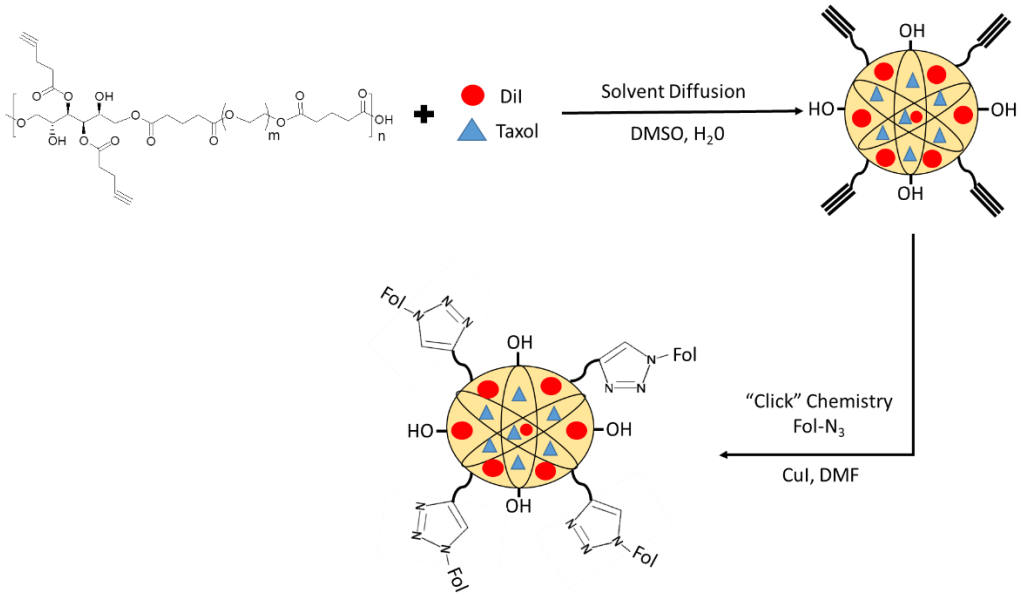

Figure 20: Conversion of Polymer to Nanoparticles and Surface Ligand Modification

DLS and Zeta Potential Determination: Following cargo encapsulation, folate modification and dialysis, the nanoparticles were subjected to Dynamic light scattering (for diameter determination) and surface charge (zeta potential) determination. Zeta potential determination is a technique somewhat exclusive to nanotechnology, which measures the potential difference between the surface of a particle immersed in a conducting liquid and the bulk of the liquid. This is important to gauge, as it allows one to monitor the success of surface modification via changes in the overall surface charge of the nanoparticles. Since cell membranes possess a negative charge, it is important to produce nanoparticles with either overall positive surface charge or receptor-specific ligands. The results of both analyses are shown in Figures 21-24.

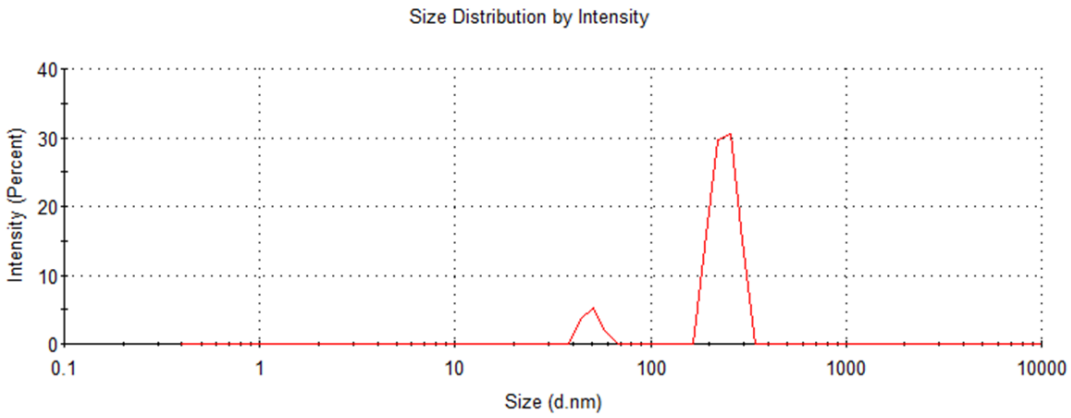

Figure 21: DLS of PEG-300 PNPs

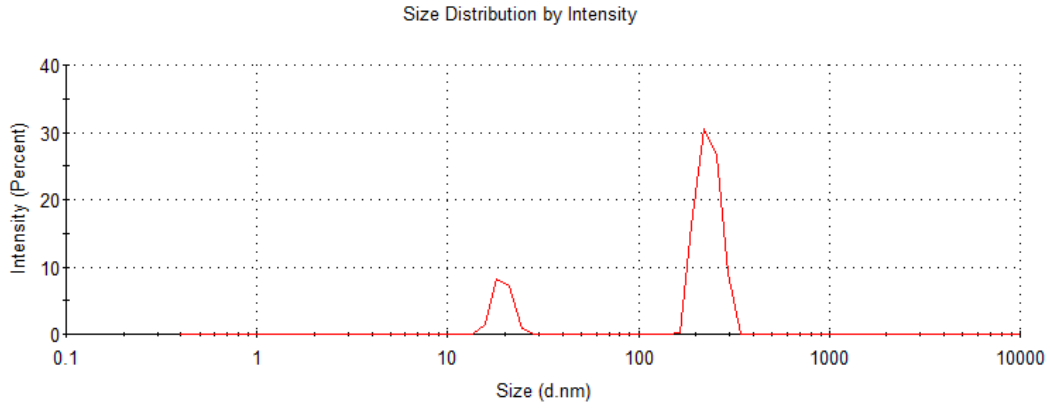

Figure 22: DLS of PEG-300 PNPs

The analysis showed two types of PEG-300 polymeric nanoparticles, with diameters 49.90 nm to 240.0 nm, comprising 10.7% and 89.3% of the sample, respectively. The PEG-1000 polymeric nanoparticles displayed particles with 19.43 nm and 233.7 nm diameters, comprising 17.7% and 82.3% of the sample, respectively. It is likely that the larger particles were agglomerates of multiple nanoparticles, which may occur as the samples remain undisturbed for long periods (around 3-7 days).[29] Despite this, these sizes are within acceptable ranges for usage in targeted drug delivery in-vitro, since nanoparticles exceeding 500 nm in diameter suffer from issues with receptor binding and cellular uptake.[19-20]

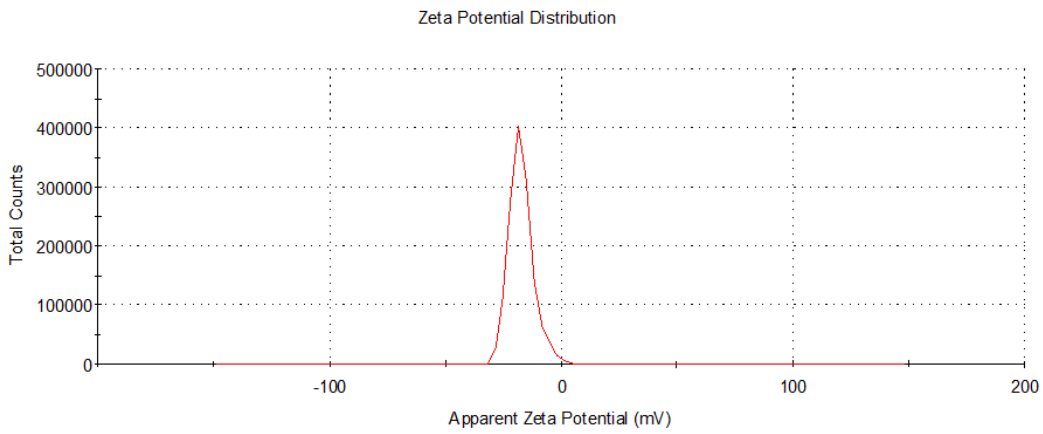

Figure 23: Average Surface Zeta Potential of PEG-300 PNPs

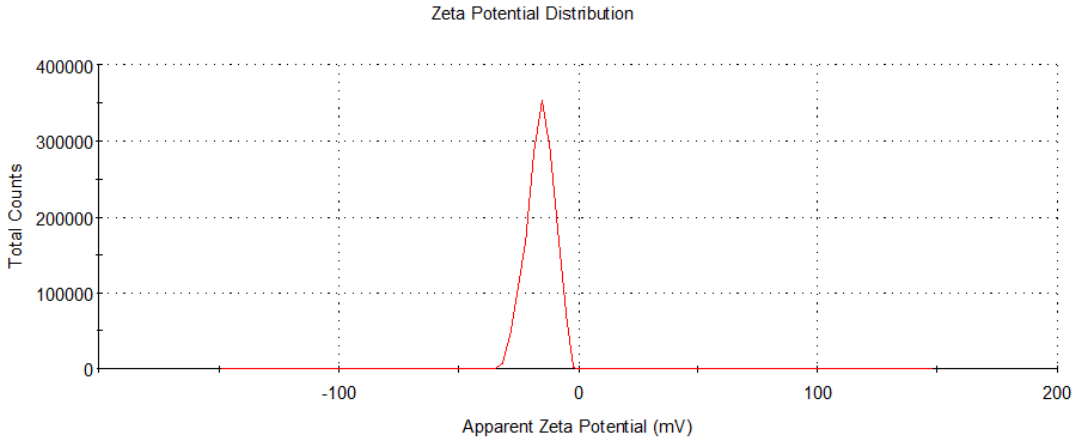

Figure 24: Average Surface Zeta Potential of PEG-1000 PNPs

The results of the surface zeta potential show average vales of -18.7 mV and -19.8 mV for the PEG-300 and PEG-1000 polymeric nanoparticles, respectively. These values were expected, as the carbonyl oxygens present in the 4-pentynoic acid surface pendants and the secondary alcohols in the sorbitol component of the polymer would result in an overall negative charge. These relatively low charge values may also play a part in the larger diameters seen in both samples, as the attractive forces may exceed repulsive ones.[29-30] These values matter little

in the nanoparticle's ability to be taken up by the cells, however, as they will eventually be modified for folate receptor targeting, which supersedes the surface charge of the molecules.

Nanoparticle Absorbance and Fluorescence: Following encapsulation of DiI and surface decoration with folic acid, the nanoparticles were analyzed by absorbance and fluorescence spectroscopy. This was performed to determine the presence of DiI dye and folic acid after the completion of synthesis and dialysis, as well as to determine if they maintained their activities after encapsulation. The results of these analyses are shown in Figures 25 and 26.

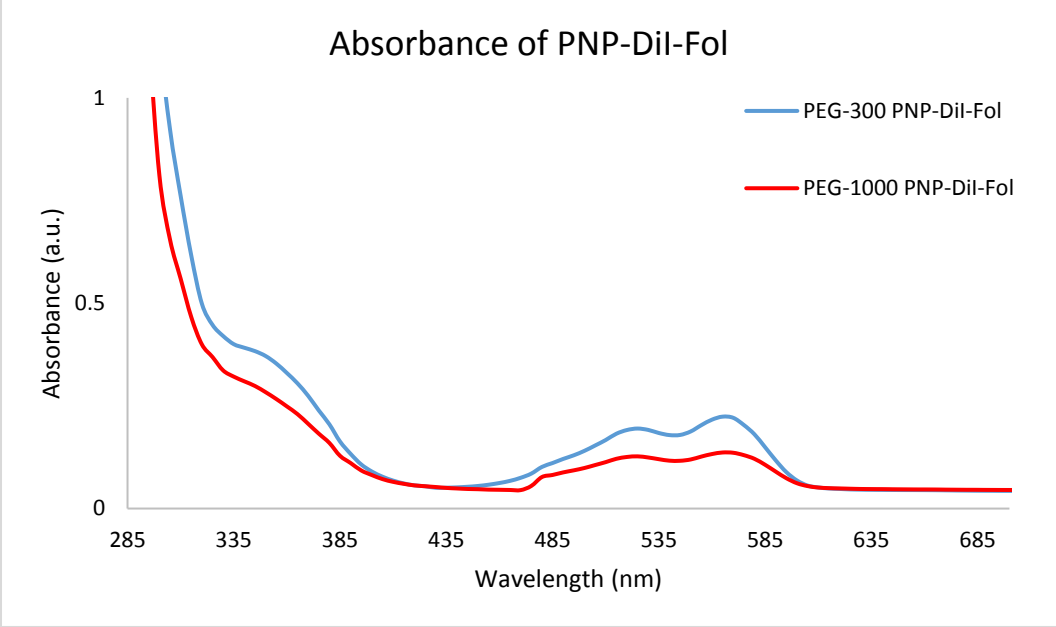

Figure 25: Absorbance of PNPs with Encapsulated DiI Dye

The absorbance spectra for the PNPs showed absorbance at 350 nm and in the 520-560 nm range, indicative of folic acid and DiI, respectively. This indicated that the cargo molecules were present within the nanoparticles and the folic acid ligands conjugated to the surface maintained their absorbance through the synthesis and purification. The somewhat broadened absorbance for DiI was likely due to the polymer matrix and the media (deionized water) in

which the nanoparticles were suspended, which can cause absorbance to deviate slightly from the expected values.

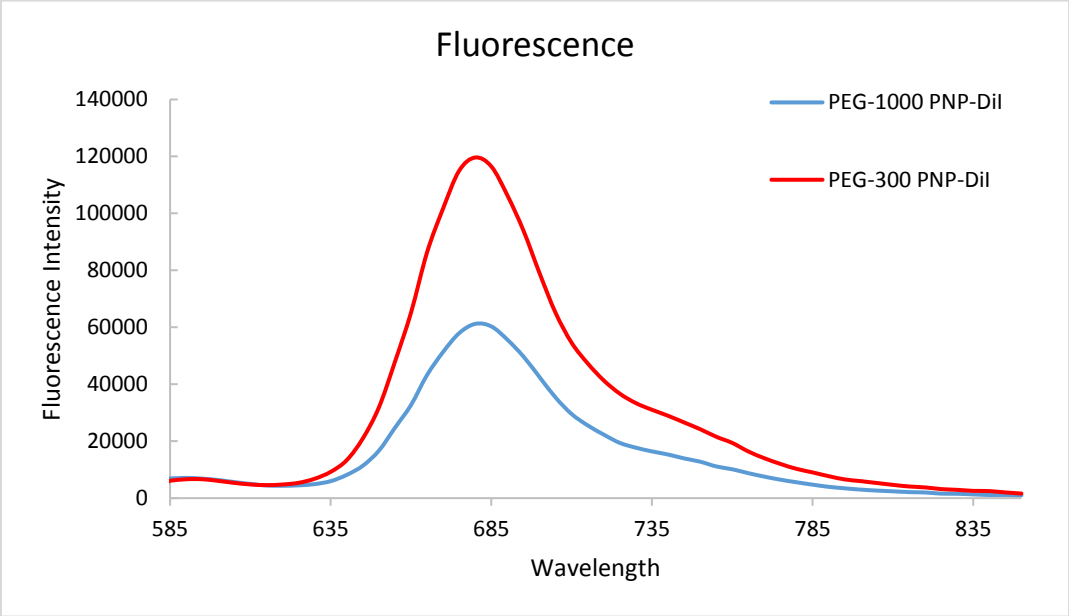

Figure 26: Fluorescence Emission of PNPs with Encapsulated DiI Dye

The fluorescence emission spectra showed the characteristic peak for DiI in the range of 650 to 700 nm. As mentioned before, the broadening of the peak beyond this range was attributed to the deionized water in which the nanoparticles were dispersed. Regardless, the results showed that the dye maintains its fluorescence activity within the nanoparticle. This would suggest that this nanoparticle system would be suitable for fluorescence imaging that would show real-time progress of the effects of therapeutics on the treated cells.

3. Cell Culturing and Cytotoxicity Assay

MTT Assay: To determine the efficiency of the nanoparticle's cellular uptake and cytotoxicity, the cells were subjected to an MTT assay. LNCaP and PC3 prostate cancer cells were cultured in a 96-well plate and incubated with 50 µL each of (1) PNP-DiI and (2) PNP-DiI-Fol and (3) PNP-DiI-Fol-Tax from both nanoparticle samples. A well for untreated (control) cells

were also cultivated for comparative purposes. The nanoparticles were permitted 24 hours of incubation (with results assessed at 6, 12 and 24 hours) within a humidified incubator at 37°C and 5% CO_2 atmosphere. After the incubation, the cells were treated with the MTT/ Phosphate-buffered saline (PBS) solution and incubated for an additional 4-6 hours. The apoptotic effects of the treatment are measured with respect to the absorbance intensities of the MTT compound (560 nm). The cumulative results of these experiments are detailed in Figure 27 and 28.

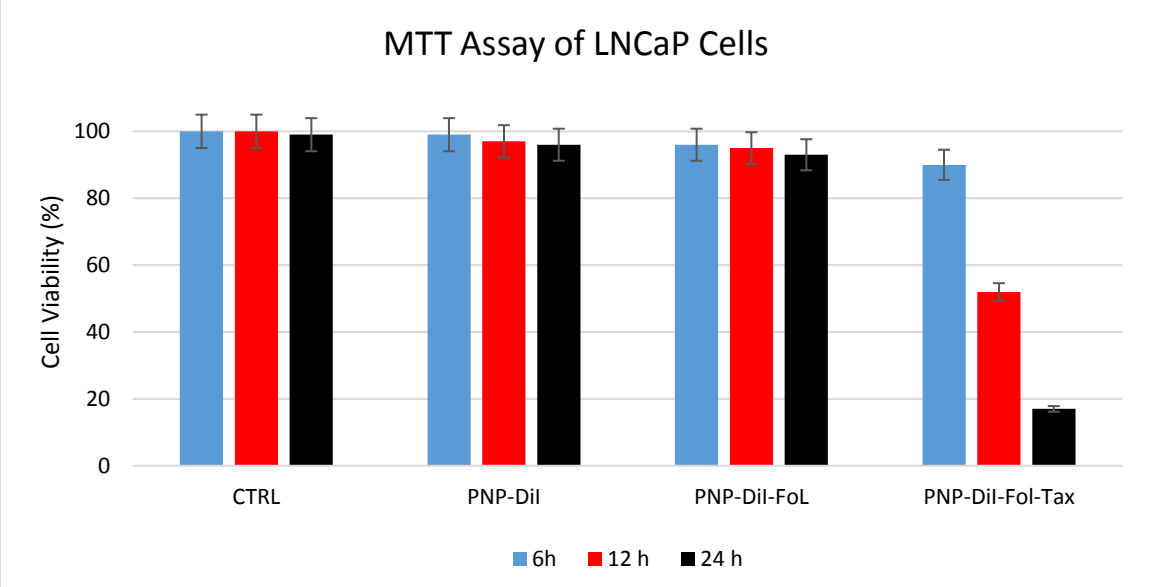

Figure 27: Cytotoxicity Effects of PNPs on LNCaP Prostate Cancer Cells

Figure 27 revealed that the folate-functionalized nanoparticles carrying Taxol displayed significant cytotoxicity to LNCaP cells, killing approximately 50% of the cells after only 12 hours of incubation. Those subjected to 24 hours of incubation displayed approximately 80% cell death. Conversely, nanoparticles lacking the encapsulated Taxol did not display reduction in cell viability. This suggested that our functionalized nanoparticles encapsulating anticancer drugs entered these cells and degraded, releasing Taxol to the cytosol and initiated apoptosis.

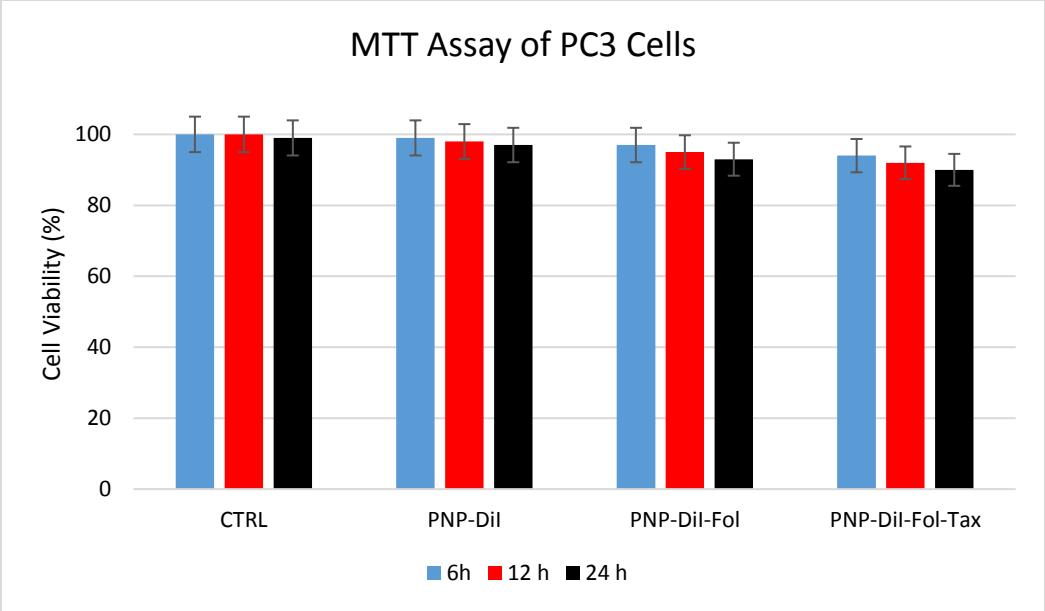

Figure 28: Cytotoxicity Effects of PNPs on PC3 Prostate Cancer Cells

This assay was also performed on PC3 prostate cancer cells to gauge the selectivity of our functionalized nanoparticles, as these cells lack the PSMA receptor. As seen in the results for the PC3 MTT assay, no significant cell death was observed in any of the trails. This was due to PC3 cells' lack of the PSMA receptor expressed in the LNCaP cell line, which displays a high affinity for folic acid. This provided evidence that our functionalized nanoparticles were selective for cell lines expressing the PSMA receptor, as significant cytotoxicity was only observed in the LNCaP cells. The slight reduction in PC3 cell viability observed at longer incubation times was attributed to disruption of the media (e.g. slight changes in pH) as exposure to nanoparticles increased.

CHAPTER IV

CONCLUSION

A synthetic, hydrophilic polyester polymer was synthesized using biocompatible monomers. The various characterizations of the polymer showed a compound with high molecular weight, thermostability, and alkyne surface functionality that permitted further modification as a drug delivery system. The polymer was successfully converted into a polymeric nanoparticle suspension, possessing nano-scale diameters and alkyne surface functionalities that were further modified by “click” chemistry. The nanoparticles also successfully encapsulated the optical dye and anti-cancer drug while remaining stable at physiological conditions. Cytotoxicity assays showed the nanoparticle’s efficacy and specificity for LNCaP prostate cancer, killing around 80% of these cells after 24 hours of incubation.

Looking forward, fluorescent microscopy on the cells following treatment need to be conducted, as this presents another means to track the progression of therapy. Microscopy is more applicable to the biological and medical aspects of this project, but also makes the results of therapy observable for more qualitative analysis. Release studies also need to be performed on the polymeric nanoparticles, dialyzing them in the presence of esterase and varying pH levels. This would aid in determining the amount of cargo molecules released into the cells over time, as well as elucidating other types of conditions the nanoparticles can endure. Finally, modification of the protocol for use in in-vivo mice models expressing prostate cancer needs to

be considered. This would entail synthesizing nanoparticles with even smaller diameters (below 10 nm), as the sizes obtained in this project may be incompatible in living models. Observation of the qualities of the polymers created from lower reaction times (24 hours or less) to determine if they could provide particles of smaller diameters is also a topic of interest.

CHAPTER V

EXPERIMENTAL METHODS

Materials

The near-infrared fluorescent dye 1,1'-Dioctadecyl-3,3,3',3'-tetramethylindocarbocyanine perchlorate (DiI) and the chemotherapeutic drug Paclitaxel (Taxol) were purchased from Invitrogen and ThermoFisher, respectively. Deuterated dimethyl sulfoxide (DMSO-d_6) and chloroform ($CDCl_3$) for use in ^{1}H NMR and ^{13}C NMR spectroscopy were purchased from Sigma-Aldrich. The various solvents used for solubility determination (methanol, dimethyl sulfoxide, tetrahydrofuran, and toluene) of the polymers were purchased from Sigma-Aldrich or Acros Organics and used as received. Sorbitol, glutaric acid, PEG-1000, and 4-pentynoic acid were purchased from Sigma Aldrich and used without further purification. 3-(4,5-dimethylthiazol-2-yl)-2,5-diphenyltetrazolium bromide (MTT), and 4' 6-diamidino-2-phenylindole (DAPI) were purchased from Biotium. LNCaP and PC3 prostate cancer cells were obtained from the American Type Culture Collection (ATCC) organization and cultured per their supplied protocol.

Polyester Polymer Synthesis

Sorbitol (1.38 g, 7.57 mmol), glutaric acid (2.0 g, 15.14 mmol), 4-pentynoic acid (0.371g, 3.78 mmol) and either polyethylene glycol 1000 (7.57 g, 7.57 mmol) or polyethylene 300 (2.27 g, 7.57 mmol) were added to a 50 mL round-bottom flask containing a stir bar, then placed in an

oil bath heated to 110°C until all the compounds had melted. After melting, the temperature was reduced to 95°C and Novozyme-435 (400 mg), a lipase catalyst used for esterification at lower temperatures below 100°C, was added to the melt. The flask was topped with a vacuum adapter, attached to a Schlenk line, and flushed with nitrogen gas (99.99% purity) to create an inert atmosphere. The reaction proceeded for 12 hours under nitrogen atmosphere, after which the mixture was treated with a high vacuum ($4x10^{-4}$ mm/Hg). The vacuum exposure (applied to remove the water byproduct and drive the reaction to completion) lasted 72 hours, with two 2-3 g samples taken at 48 and 72 hours of total reaction time.

To purify the polymer, each sample was dissolved in methanol and filtered through P8-grade (fine) filter paper to isolate the polymer solution from the expended catalyst. The isolated sample was placed in 50 mL round-bottom flask and subjected to rotary evaporation (low vacuum and 60°C) to remove the methanol. If necessary, the samples were subjected to direct high vacuum to further ensure the complete removal of methanol. The purified PEG-300 polyester polymer possessed a molasses-like texture and viscosity, while the PEG-1000 polyester polymer was more wax-like. Both the 48 and 72 hr. samples of the PEG-300 and PEG-1000 polymers were found to be soluble in water, dimethyl sulfoxide (DMSO), chloroform ($CHCl_3$), dimethyl formamide (DMF) and tetrahydrofuran (THF).

Polymeric Nanoparticle Synthesis

The polymer (30 mg) was placed in an Eppendorf tube and dissolved in DMSO (250 µL). Then DiI optical dye (2 µL) and Taxol (2 µL) were added to the polymer solution and vortexed for approximately 3 minutes at 1500 rpm. The resulting mixture was slowly added dropwise (8 µL aliquots) to a 15-mL centrifuge tube containing deionized water (4 mL) with continuous vortexing. Once the polymer-cargo mixture has been completely added to the water, the

centrifuge tube was capped and the vortex speed increased to 2500 rpm. The drug and dye-encapsulating nanoparticle exhibited a faint pink color (indicative of encapsulated DiI) and was devoid of precipitate. The mixture was then transferred to a porous dialysis sleeve (MWCO= 3-6 kDa) for dialytic purification in deionized water for 1 hour.

Folic Acid Conjugation

Further modification of the surface functional groups was necessary for selective treatment of LNCaP prostate cancer cells. Due to the presence of C≡C surface functional groups, the nanoparticles were amenable to "click" chemistry with azide-functionalized folic acid (Fol-N3). The addition of the folate ligand allows for selective uptake by LNCaP cells, which are known to overexpress folate receptors at the cell membrane exterior. The synthesis and preparation for Fol-N3 is detailed in the following section and in Figure 29.

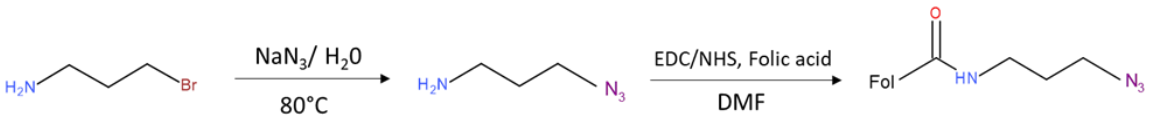

Figure 29: Synthesis of Azide-Functionalized Folic Acid

Modification of the folic acid begins with the synthesis of aminopropyl azide. This is accomplished by adding 3-bromopropyl amine (7 g, 0.051 mol) and of sodium azide (14.23 g, 0.219 mol) to a 100 mL roundbottom flask containing deionized water (40 mL), which is then heated to 80°C for 20 hours. Thereafter, solvent was removed in a rotary evaporator under low vacuum, followed by the addition of potassium hydroxide (2 g, 0.036 mol) and extraction with petroleum ether.

For the next sequence in the synthesis, folic acid (0.05 g, 0.113 mmol) was dissolved in DMSO (2 mL). In a separate vial, of 1-Ethyl-3-(3-dimethylaminopropyl) carbodiimide (EDC) (0.02 g, 0.129 mmol) and N-Hydroxysuccinimide (NHS) (0.013 g, 0.113 mmol) were combined in 2-(N-morpholino) ethanesulfonic acid (MES) Buffer (0.5 mL, pH 5.0). Both solutions were combined and allowed to incubate at room temperature for 3 minutes. Following the brief incubation, aminopropyl azide (0.007 g, 0.07 mmol) was dissolved in PBS (0.025 mL), added dropwise to the mixture, and incubated for an additional 3 hours. Lastly, the solution was centrifuged at 5000 RPM and the azide-functionalized folic acid supernatant collected and dissolved in DMF (1 mL) until further use.

To complete the bonding to the nanoparticles, nanoparticle suspension (2 mL) in a bicarbonate buffer (pH=7.4) was combined with the azide-functionalized folic acid dissolved in DMF (0.02 mol). Copper iodide (0.001 mmol) in DMF (5 µL) was added to the mixture and incubated at room temperature for 12 hours on a table mixer, after which the reaction mixture was purified by dialysis in deionized water, and stored at 4°C until further use.

Instrumentation

^{1}H NMR: Samples of each monomer (5-10 mg) or polymer (50 mg) were dissolved in DMSO-d_6 or chloroform-d (1 mL). The samples were processed in the Bruker DPX-300 MHz spectrometer using the TOPSPIN 1.3 program for 25 scans. Polymer samples were vacuum-dried before dissolving in the deuterated solvent.

^{13}C NMR: Samples of each monomer and polymer (40-50 mg) were dissolved in DMSO-d_6 (1 mL). The samples were processed in the Bruker DPX-300 MHz spectrometer using the TOPSPIN 1.3 program for 1000 scans. Polymer samples were vacuum-dried before dissolving in the deuterated solvent.

FT-IR: Monomer or polymer samples (1- 5 mg) were placed in the PerkinElmer Spectrum 2 FT-IR spectrometer and scanned to gain their respective spectra. Polymer samples were vacuum-dried and desiccated before analysis.

Gel Permeation Chromatography (**GPC**)**:** Gel permeation chromatography (GPC) was performed with a Waters 2410 DRI gel permeation chromatograph, consisting of four phenogel 5 µL columns filled with cross-linked polystyrene-divinylbenzene (PSDVB) beads. The polymer samples (5 mg) were first vacuum-dried, dissolved in THF (1 mL), then transferred to a GPC vial. The flow rate of tetrahydrofuran (THF) eluent was set to 1 mL/min at 25^{o}C for 50 minutes.

Thermogravimetric Analysis (**TGA**): The thermal stability of the polymer was tested on a TA Instruments Q50 thermogravimetric analyzer. Polymer samples of about 5 mg were weighed, equilibrated, and then heated under nitrogen atmosphere using a heating ramp of 10°C/min for 60 minutes, ranging from 25 to 600°C.

Differential Scanning Calorimetry (DSC): The calorimetric parameters of the polymer were gauged on a TA Instruments Q100 differential scanning calorimeter. Polymer samples of about 7-8 mg were used for the test. The device was set to run three cycles ranging from -70°C to 160°C, with a ramp of 10°C/min. The beginning of each cycle was precluded by a three-minute isothermal period, after which the ramping would begin again.

Matrix-Assisted Laser Desorption/Ionization-Time of Flight (MALDI-TOF): Analysis was performed on the Bruker microflex™ LRF MALDI-TOF. The matrix for the samples was prepared per protocol in the Bruker user manual. First, TA30 solvent (30:70 volume ratio of acetonitrile to 0.1% trifluoroacetic acid) was prepared in 100 µL quantity. Then 2,5-dihydroxybenzoic acid (2 mg) was thoroughly dissolved and mixed in the TA30 to complete the matrix. Next, the polymer sample (5 mg) was vacuum dried, desiccated, and then dissolved in methanol (100 mL). The

polymer solution and TA30 matrix were then combined into a single Eppendorf tube and vortexed (1000 rpm) for 2 minutes to ensure complete mixing. The resulting solution was then spotted (1 µL drop size) in the wells of a ground steel MALDI target plate. The spots were left to dry completely (approx. 6 hours) and placed in the mass spectrometer for analysis.

Dynamic Light Scattering and Zeta Potential: The polymeric nanoparticle (10 µL) solution was added to deionized water (1 mL). This solution was then placed in a standard cuvette for DLS reading, or a specialized electrode-containing cuvette for zeta potential determination. The appropriate cuvette was placed in the Malvern ZS90 zetasizer and the program set up (approximately 50 readings in 3 cycles) for the appropriate data acquisition.

Uv/Vis and Fluorescence Analysis: UV/Vis spectra were recorded using a Tecan infinite M200 Pro microplate reader. Samples of polymeric nanoparticle suspension (50 µL) were placed in the wells of a 96-well plate and placed in the spectrophotometer. Absorbance scans were set to read a range of 300-800 nm, while fluorescence emission scans were set to read wavelengths of 600-900 nm. Readings were taken at intervals of 5 nm, with 10 flashes for each reading. The resulting data points were transferred to Microsoft Excel and plotted to visualize and compare the two samples.

Cell Studies

Cell Culturing: LNCaP and PC3 prostate cancer cells were grown in a specially formulated media containing, by volume, 85% RPMI-1640 media, 10% fetal bovine serum, and 5% Penicillin/Streptomycin antibiotic. These components were mixed, vacuum-filtered, and stored at 4°C until needed. The cells taken from cryo were re-suspended in this media (5 mL), transferred to a 7-mL culture flask, and incubated at 37°C. Cells were split to new flasks with fresh media as needed to prevent overcrowding and to increase the longevity of the cells. Cell samples used for

assays were taken from flasks with the most recently changed media and at least 24 hours old, or roughly 80% confluent.

MTT Assay: Fresh cells were cultured in a 96-well plate and incubated with 50 µL dosages of the polymeric nanoparticle formulations (both with and without folic acid and Taxol) for 24 hours. Following the incubation, the media was removed and 50 µL of 1X PBS was added to the cells for washing. The PBS was removed, then 25 µL of the MTT solution (50 mg MTT in 10 mL 1X PBS) is added to the wells and incubated for 4-6 hours. After incubation, the excess MTT solution was drained from the wells, then 30 µL of isopropanol added. The cells then were ready to be read in the TECAN Infinite M200 PRO multi-detection microplate reader (at 560 nm absorbance) to determine the efficacy of nanoparticle treatment.

REFERENCES

1. Paris G, Berlinguet L, Gaudry R, English J. and Dayan JE (1963). "Glutaric Acid and Glutaramide". *Org. Synth. Coll*. **4**, 496.
2. Teo, G; Suzuki, Y; Uratsu, SL; Lampinen, B; Ormonde, N; Hu, WK; Dejong, TM; Dandekar, AM (2006). "Silencing leaf sorbitol synthesis alters long-distance partitioning and apple fruit quality". *Proceedings of the National Academy of Sciences of the United States of America.* **103** (49): 18842–7.
3. "Polymer". *The Free Dictionary*. Farlex. http://www.thefreedictionary.com/polymer. (Accessed Apr 5, 2017).
4. "Monomer". *The Free Dictionary*. Farlex. http://www.thefreedictionary.com/monomer. (Accessed Apr 5, 2017).
5. Staudinger, H (1920). "Über Polymerisation". *Ber. Deut. Chem. Ges.* **53** (6): 1073.
6. Mülhaupt, R (2004). "Hermann Staudinger and the Origin of Macromolecular Chemistry". *Angew*. Chem. Int. Ed. **43** (9): 1054–1063.
7. Staudinger, H (1933). "Viscosity investigations for the examination of the constitution of natural products of high molecular weight and of rubber and cellulose". *Trans. Faraday Soc*. **29** (140): 18–32.
8. "Herman Mark and the Polymer Research Institute". *National Historic Chemical Landmarks. American Chemical Society*. Retrieved 2015-12-01. (Accessed Apr 5, 2017).
9. Hermes, Matthew. *Enough for One Lifetime: Wallace Carothers, Inventor of Nylon. Chemical Heritage Foundation*, 1996.
10. Ikada Y, Tsuji H (2000). "Biodegradable polyesters for medical and ecological applications." *Macromol. Rapid Commun*. **21**, 117-132.
11. Vroman I, Lan T (2009). Biodegradable Polymers. *Materials*. **2** (2), 307-344.
12. Chandra R, Rustgi R (1998). "Biodegradable polymers". *Progress in Polymer Science.* **23**(7), 1273-1335.
13. Lee C, Hong S (2014). "An Overview of the Synthesis and Synthetic mechanism of Poly(Lactic acid)". *Mod. Chem. Appl*. **2**, 144.
14. Robergs RA, Ghiasvand F, Parker D (2004). "Biochemistry of exercise-induced metabolic acidosis". *Am. J. Physiol. Regul. Integr. Comp. Physiol*. **289** (3): R890-94.

15. Nanjwade BK, Bechra HM, Derkar GK, Manvi FV, Nanjwade VK (2009). "Dendrimers: Emerging polymers for drug-delivery systems". *European Journal of Pharmaceutical Sciences*. **38** (3), 185–196.
16. Santra S, Kaittanis C, Manuel Perez J (2010). "Aliphatic Hyperbranched Polyester: A New Building Block in the Construction of Multifunctional Nanoparticles and Nanocomposites". *Langmuir*. **26** (8), 5364-5373.
17. Fu L, Cheng X, Zhang Z, Zhuo R (2008). "Dendrimer/DNA complexes encapsulated functional biodegradable polymer for substrate-mediated gene delivery". *The Journal of Gene Medicine*. **10** (12), 1334–1342.
18. Campos B, Algarra M, Esteves da Silva J (2010). "Fluorescent Properties of a Hybrid Cadmium Sulfide-Dendrimer Nanocomposite and its Quenching with Nitromethane". *Journ. of Fluor*. **20** (1), 143–151.
19. Santra S, Kaittanis C, Manuel Perez J (2010). "Cytochrome *c* Encapsulating Theranostic Nanoparticles: A Novel Bifunctional System for Targeted Delivery of Therapeutic Membrane-Impermeable Proteins to Tumors and Imaging of Cancer Therapy". *Mol. Pharm*. **7** (4), 1209-1222.
20. Santra S, Manuel Perez J (2011). "Selective N-Alkylation of β-Alanine Facilitates the Synthesis of a Poly(amino acid)-Based Theranostic Nanoagent". *Biomacromol*. **12**, 3917-3927.
21. Zwicke G, Mansoori G, Jeffery C (2012). "Utilizing the folate receptor for active targeting of cancer nanotherapeutics". Nano Rev. **3**: 18496.
22. Sheehan J, Cruickshank P, Boshart G (1961). "A Convenient Synthesis of Water-Soluble Carbodiimides". *J. Org. Chem*. **26** (7): 2525.
23. Kolb H, Finn M, Sharpless K (2001). "Click Chemistry: Diverse Chemical Function from a Few Good Reactions". *Angewandte Chemie International Edition*. **40** (11): 2004–2021.
24. Mosmann T (1983). "Rapid colorimetric assay for cellular growth and survival: application to proliferation and cytotoxicity assays". *J. of Immun. Meth*. **65** (1-2): 55-63.
25. Berridge MV, Tan AS (1993). Characterisation of the cellular reduction of 3-(4,5-dimethylthiazol-2yl)-2,5-diphenyltetrazolium bromide (MTT): Subcellular localization, substrate dependence, and involvement of mitochondrial electron transport in MTT reduction. *Archives Biochem Biophys.* **303**: 474-482.

26. Sperling L, Pearson RA (2011). "The Amorphous State." Introduction to Physical Polymer Science. Hoboken: Wiley-Blackwell.
27. “Dipolar Aprotic Solvent”. *IUPAC Compendium of Chemical Terminology*. International Union of Pure and Applied Chemistry. http://goldbook.iupac.org/html/D/D01751.html. (Accessed April 20, 2017).
28. Santra S, Manuel-Perez J (2011). Selective N-Alkylation of β-Alanine Facilitates the Synthesis of a Poly(amino acid)-Based Theranostic Nanoagent”. *Biomacromolecules*. **12**: 3917-3927.
29. Greenwood R, Kendall K (1999). “Electroacoustic studies of moderately concentrated colloidal suspensions”. *Journal of the European Ceramic Society*. **19**(4): 479-488.
30. Hanaor, D.A.H.; Michelazzi, M.; Leonelli, C.; Sorrell, C.C. (2012). "The effects of carboxylic acids on the aqueous dispersion and electrophoretic deposition of ZrO_2". *Journal of the European Ceramic Society*. **32** (1): 235–244.